

1 **Exploration of Enceladus and Titan: Investigating Ocean Worlds' Evolution and**  
2 **Habitability in the Saturn System**

3 <sup>1,2</sup>Mitri, Giuseppe, <sup>3</sup>Barnes Jason, <sup>4</sup>Coustenis Athena, <sup>1</sup>Flamini Enrico, <sup>5</sup>Hayes Alexander, <sup>6</sup>Lorenz  
4 Ralph D., <sup>7</sup>Mastrogiuseppe Marco, <sup>8</sup>Orosei Roberto, <sup>9</sup>Postberg Frank, <sup>10</sup> Reh Kim, <sup>11</sup>Soderblom  
5 Jason M., <sup>10</sup>Sotin Christophe, <sup>12</sup>Tobie Gabriel, <sup>13</sup>Tortora Paolo, <sup>14</sup>Vuitton Veronique, <sup>15</sup>Wurz Peter  
6

7 <sup>1</sup>International Research School of Planetary Sciences, Università d'Annunzio, Italy  
8 (giuseppe.mitri@unich.it)

9 <sup>2</sup>Dipartimento di Ingegneria e Geologia, Università d'Annunzio, Italy

10 <sup>3</sup>University of Idaho, USA

11 <sup>4</sup>LESIA, Observatoire de Paris, France

12 <sup>5</sup>Cornell University, USA

13 <sup>6</sup>JHU Applied Physics Lab., USA

14 <sup>7</sup>Università La Sapienza, Italy

15 <sup>8</sup>INAF, Italy

16 <sup>9</sup>University of Heidelberg, Germany

17 <sup>10</sup>Jet Propulsion Laboratory, USA

18 <sup>11</sup>Massachusetts Institute of Technology, USA

19 <sup>12</sup>Université de Nantes, France

20 <sup>13</sup>University of Bologna, Italy

21 <sup>14</sup>Univ. Grenoble Alpes, CNRS, CNES, IPAG, France

22 <sup>15</sup>University of Bern, Switzerland

23 **Corresponding author:**  
24 Giuseppe Mitri  
25 International Research School of Planetary Sciences  
26 Dipartimento di Ingegneria e Geologia  
27 Universita' d'Annunzio  
28 Viale Pindaro 42  
29 65127 Pescara Italy  
30  
31 Office: +39.085.453.7306  
32 Email: [giuseppe.mitri@unich.it](mailto:giuseppe.mitri@unich.it)

33 **Abstract**

34 We present a White Paper with a science theme concept of ocean world evolution and habitability  
35 proposed in response to ESA’s Voyage 2050 Call with a focus on Titan and Enceladus in the  
36 Saturn system. Ocean worlds in the outer Solar system that possess subsurface liquid water oceans  
37 are considered to be prime targets for extra-terrestrial life and offer windows into Solar System  
38 evolution and habitability. The Cassini Huygens mission to the Saturn system (2004–2017)  
39 revealed Titan with its organic-rich evolving world with terrestrial features and Enceladus with its  
40 active aqueous environment to be ideal candidates to investigate ocean world evolution and  
41 habitability. Additionally this White Paper presents a baseline for a multiple flyby mission with a  
42 focused payload as an example of how ocean world evolution and habitability in the Saturn system  
43 could be investigated building on the heritage of the Cassini-Huygens mission and complementing  
44 the recently selected NASA Dragonfly mission.

45

46

47 **Executive summary**

48 Recent observations from the ground and in space have shown that Earth is not the only place in  
49 the Solar System to possess exposed surface liquid. Observations have provided evidence of  
50 subsurface liquid water oceans covered by icy shells on multiple objects in the Solar System, called  
51 ocean worlds, including the icy moons of Jupiter (Europa, Ganymede and Callisto) and of Saturn  
52 (Titan and Enceladus) as well as dwarf planets (Ceres and Pluto) (see Lunine 2017 for a review  
53 and De Sanctis et al., 2020). The Cassini-Huygens mission has shown Titan and Enceladus to be  
54 two favourable locations in the Solar System in our quest for a better understanding of the  
55 evolution of the Solar System and its habitable potential. Both Saturnian moons possess energy

56 sources, liquid habitats, nutrients (organic compounds) and transport cycles of liquid moving  
57 nutrients and waste, all necessary ingredients for habitability (McKay, 2016; Hand et al. 2020).  
58 Titan is the only active extraterrestrial alkanological system in the Solar System (analogous to the  
59 Earth's hydrological system), including an organically rich atmosphere, hydrocarbon lakes and  
60 seas on the surface and a liquid water subsurface ocean. Enceladus has active plumes composed  
61 of multiple jets containing complex organics and water vapour and likely connected to its liquid  
62 water subsurface ocean. Along with their energy sources, these bodies are prime environments in  
63 which to investigate the conditions for the emergence of life and habitability conditions of ocean  
64 worlds in the Outer Solar System, as well as the origin and evolution of gas giant planetary  
65 systems, in a single mission.

66

67 We propose a Voyage 2050 theme of ocean worlds evolution and habitability with a focus on  
68 Enceladus and Titan in the Saturn system. Building on the heritage of Cassini-Huygens, future  
69 exploration of Enceladus and Titan should be dedicated to investigating the unique properties and  
70 the habitability potential of these ocean worlds. The proposed baseline is for a large mission (class  
71 L) and consists of multiple flybys using a solar-electric powered spacecraft (S/C) in orbit around  
72 Saturn. The proposed mission would have a focused payload that would provide high-resolution  
73 mass spectrometry of the plume emanating from Enceladus' south polar terrain and of Titan's  
74 upper atmosphere. High-resolution IR imaging would be performed of the plume and the source  
75 fractures on Enceladus' south polar terrain (SPT), and would detail Titan's geomorphology at 50–  
76 100 m resolution at minimum. In addition, radio science measurements would provide constraints  
77 on the ice shell structure and the properties of the internal ocean of Enceladus and constrain higher  
78 degree gravity field components of Titan. The baseline mission is based on the Explorer of

79 Enceladus and Titan (E<sup>2</sup>T) concepts proposed as a medium-class mission led by ESA in  
80 collaboration with NASA in response to ESA's M5 Call (Mitri et al., 2018), along with several  
81 other previous proposals (e.g. TSSM, Coustenis et al. 2009; TIME, Stofan et al. 2010; JET, Sotin  
82 et al. 2011) and will complement the information provided by Cassini-Huygens, as well as the  
83 results of the newly-selected NASA Dragonfly mission.

84  
85 The baseline mission can address key scientific questions regarding extraterrestrial habitability,  
86 abiotic/prebiotic chemistry, the emergence of life, and the origin and evolution of ocean worlds.  
87 Optional elements include a) an *in-situ* sea-probe to investigate one of Titan's northern seas as  
88 well as the lower atmosphere and b) an ice penetrating radar (IPR) to perform radar sounding of  
89 the subsurface of Titan and Enceladus during flybys. The *in-situ* sea-probe would open up new  
90 vistas regarding Titan's seas and lakes, the hydrological system and the possibility of  
91 prebiotic/biotic components within Titan's seas, complementing the equatorial investigations of  
92 NASA's Dragonfly, while the IPR would reveal subsurface structures and processes of Titan and  
93 Enceladus' SPT. While the baseline mission is conceived as a multiple flyby mission it can also  
94 include a final orbiter phase around Titan. The joint exploration of these two fascinating objects  
95 would potentially be performed with international collaboration and will allow us to better  
96 understand the origin of their organic-rich, liquid water habitable environment and will give access  
97 to planetary processes that have long been thought unique to the Earth. Finally, joint exploration  
98 of these ocean worlds would complement NASA's Dragonfly mission to Titan, which while  
99 unprecedented is only regional in scope exploring a low-latitude impact crater site (Selk impact  
100 crater). Thus, local observations of Enceladus' south pole, global observations of Titan and

101 possible *in-situ* exploration of a northern sea are important science goals that remain to be  
102 addressed by a future mission to the Saturn system.

103

## 104 **1. Introduction**

### 105 **1.1 Overview**

106 The NASA/ESA/ASI Cassini-Huygens mission (2004–2017) has done much to advance our  
107 understanding of Titan and Enceladus and the Saturn system in general but also introduced new  
108 first order scientific questions for geologists, astrobiologists, organic chemists, and planetary  
109 scientists, that remain unanswered to date (Dougherty et al., 2010; Coustenis et al 2015; Nixon et  
110 al. 2018; Spilker et al. 2019). On Titan, its resemblance to primitive Earth and the presence of a  
111 rich mixture of organic material in contact with liquid reservoirs, which may be in contact with  
112 the subsurface, constitute major motivations for further exploration of the astrobiological potential  
113 of this ocean world (Coustenis and Raulin, 2015). On Enceladus, the accessibility of the contents  
114 of its subsurface ocean and hydrothermal system is an unprecedented opportunity to determine its  
115 abiotic/prebiotic potential while its comet-like composition raises new questions about the  
116 evolution of the Saturnian system and the Solar System in general. In the almost 23 years since the  
117 launch of the Cassini-Huygens mission in 1997, there have been great technological advancements  
118 in instrumentation that would enable answering key questions that still remain about the Saturnian  
119 ocean worlds.

120

### 121 **1.2 Titan: An organic-rich evolving world**

122 Shrouded by a dense atmosphere of nitrogen, methane, hydrogen and haze products, Titan,  
123 Saturn’s largest satellite, was once thought to host a global ocean of methane and ethane on its

124 surface (Lunine et al., 1983). Data from the Cassini-Huygens mission uncovered a fascinating  
125 Earth-like world beneath the haze with dunes (e.g., Lorenz et al. 2006), lakes and seas (Stofan et  
126 al. 2007), networks of rivers and canyons (Tomasko et al. 2005; Soderblom et al. 2007; Poggiali  
127 et al. 2016), and mountains (Radebaugh et al. 2007; Mitri et al. 2010) and impact structures (Wood  
128 et al. 2010; Soderblom et al. 2010; Neish and Lorenz 2012; Lopes et al., 2019) within an alien  
129 landscape composed of organics and water-ice. Titan's dense, extensive atmosphere is primarily  
130 composed of nitrogen (97%) and methane (1.4%) (e.g., Bézard 2014), and a long suite of organic  
131 compounds resulting from multifaceted photochemistry which occurs in the upper atmosphere  
132 down to the surface (e.g., Israël et al. 2005; Waite et al. 2007; Gudipati et al. 2013; Bézard 2014).  
133 Titan's organic-rich dense atmosphere has provided a rich field of study with multiple models  
134 investigating the origin of its nitrogen atmosphere (e.g., Mousis et al. 2002; Miller et al. 2019), the  
135 persistence of atmospheric methane despite methane escape, and the distribution of its atmospheric  
136 components. The organics detected by the Cassini mission in Titan's atmosphere have provided  
137 tantalizing hints of the prebiotic potential of Titan's atmospheric aerosols. For example, a  
138 compelling find by Cassini for abiotic/prebiotic species is the discovery of complex large nitrogen-  
139 bearing organic molecules in Titan's upper atmosphere (Waite et al. 2007; Coates et al. 2007).  
140 Stevenson et al. (2015) suggest that membranes formed from atmospheric nitriles such as  
141 acrylonitrile could provide Titan analogues of terrestrial lipids, a component essential to life on  
142 Earth.

143

144 Since methane is close to its triple point on Titan, it gives rise to an alkanological cycle analogous  
145 to the terrestrial hydrological cycle, characterized by cloud activity, precipitation, river networks,  
146 lakes and seas covering a large fraction of the northern terrain (Figure 1) (e.g., Tomasko et al.

147 2005; Stofan et al. 2007; Mitri et al. 2007; Hayes et al. 2008). Titan is the only extraterrestrial  
148 planetary body with long-standing liquid on its surface, albeit hydrocarbons instead of water, likely  
149 fed by a combination of precipitation, surface runoff and subsurface alkanofers (hydrocarbon  
150 equivalent of aquifers) in the icy shell (Hayes et al. 2008). Recent work has shown that the surfaces  
151 of Titan's northern lakes and seas are on the same equipotential surface confirming the presence  
152 of subsurface alkanofers (Hayes et al., 2017; Mastrogiuseppe et al. 2019). Titan's seas and larger  
153 lakes are typically broad edge depressions while many small lakes present as sharp edge  
154 depressions often with raised ramparts (Birch et al. 2018) and some surrounded with rampart-like  
155 structures (Solomonidou et al. 2019). Observations of water-ice poor 5- $\mu$ m bright material  
156 surrounding Titan's northern lakes and seas may be evaporite deposits (Barnes et al. 2011); though  
157 they are also found in the largest areal concentration in equatorial regions and if they do represent  
158 evaporites, suggest previous equatorial seas (MacKenzie et al. 2014). Experimental work in Titan  
159 conditions is attempting to reveal compounds that could form evaporites on Titan and their  
160 prebiotic and biotic potential (Cable et al., 2014, 2020).

161

162

## FIGURE 1

163

164 The presence of radiogenic noble gases in the atmosphere indicates some communication between  
165 the surface and the subsurface and is suggestive of water-rock interactions and methane outgassing  
166 processes (Tobie et al. 2012), possibly associated with cryo-volcanic activity (Lopes et al. 2007;  
167 2019). The detection of a salty ocean at depth estimated between 50 and 80 km beneath the surface  
168 (Iess et al. 2012; Beghin et al. 2012; Mitri et al. 2014b) and the possible communication between  
169 this ocean and the organic-rich surface opens up exciting astrobiological perspectives. While



170 Cassini has provided tantalizing views of the surface with its lakes and seas, dunes, equatorial  
171 mountains, impact craters and possible cryo-volcanoes, its low resolutions make it difficult to  
172 identify morphological features, to quantify geological processes and relationships between  
173 different geological units and monitor changes due to geologic or atmospheric activity.  
174 Determining the level of geological activity on Titan is crucial in understanding its evolution and  
175 whether this ocean world could support abiotic or prebiotic activity.

176

### 177 **1.3 Enceladus: An active aqueous environment**

178 The discovery in 2005 of a plume of multiple jets emanating from Enceladus' south polar terrain  
179 (SPT) is one of the major highlights of the Cassini–Huygens mission (Figure 2) (Dougherty et al.  
180 2006; Porco et al. 2006; Spahn et al. 2006; Lunine et al. 2018). Despite its small size (10 times  
181 smaller than Titan), Enceladus is the most active moon of the Saturnian system. Although geyser-  
182 like plumes have been observed on Triton (Soderblom et al. 1990) and more recently transient  
183 water vapor activity around Europa has been reported (Roth et al. 2014, 2016), Enceladus is the  
184 only one proven to have current endogenic activity. Approximately 100 jets (Porco et al. 2014)  
185 form a huge plume of vapor and ice grains above Enceladus' south polar terrain and are associated  
186 with abnormally elevated heat flow along tectonic ridges, called 'tiger stripes'. Enceladus'  
187 endogenic activity and gravity measurements indicate that it is a differentiated body providing  
188 clues to its formation and evolution (Iess et al. 2014). Gravity, topography and libration  
189 measurements demonstrate the presence of a global subsurface ocean (Iess et al. 2014; McKinnon  
190 et al. 2015; Thomas et al. 2016; Čadek et al. 2016). Analysis of the gravity data showed that  
191 Enceladus' ice shell thickness above the subsurface ocean is likely 30–40 km, from the south pole  
192 up to 50° S latitude (Iess et al. 2014) while libration data suggest a mean thickness of 21–26 km

193 (Thomas et al. 2016); however recent models have shown that the variable ice shell thickness in  
194 Enceladus' south pole can be as little as 5 km (Čadek et al. 2016, 2019). This variable ice shell  
195 thickness could be the result of heat flux variation along the ice-ocean interface due to true polar  
196 wander (Tajeddine et al. 2017).

197

198

## FIGURE 2

199

200 Postberg et al. (2009) and Porco et al. (2014) have shown that most of the plume material is likely  
201 not from the upper brittle layer of the ice shell but from a subsurface liquid water reservoir beneath  
202 the icy shell. Libration measurements finally confirmed the presence of a global ocean (Thomas  
203 et al. 2016). Sampling of the plume by Cassini's instruments revealed the presence of water vapor,  
204 ice grains rich in sodium and potassium salts (Postberg et al. 2011), gas and solid phase organics  
205 (Waite et al. 2009; Postberg et al. 2008, 2015). The jet sources are connected to a subsurface salt-  
206 water reservoir that is probably alkaline in nature and the site of possible hydrothermal water-rock  
207 interactions (Porco et al. 2006, 2014; Waite et al. 2006, 2009; Postberg et al. 2009, 2011; Hsu et  
208 al. 2011, 2014; Glein et al. 2015).

209

210 The co-existence of organic compounds, salts, liquid water and energy sources on this small moon  
211 provides all the necessary ingredients for the emergence of life by chemoautotrophic pathways  
212 (McKay et al. 2008) – a generally held model for the origin of life on Earth in deep sea vents, such  
213 as the Lost City hydrothermal field located in the Mid-Atlantic Ridge. The eruption activity of  
214 Enceladus offers a unique possibility to sample fresh material emerging from subsurface liquid  
215 water and to understand how exchange processes with the interior control surface activity. It

216 provides us with an opportunity to *in situ* study phenomena that have been important in the past  
217 on Earth and throughout the outer Solar System.

218

## 219 **2. Science case after the Cassini-Huygens mission**

220 While Cassini-Huygens and its extended missions have revealed much about Enceladus and Titan  
221 (Dougherty et al. 2010; Lunine et al. 2018), the S/C was not equipped to search for life or constrain  
222 the evolution of these ocean worlds and many open questions remain. *In situ* measurements by  
223 Cassini at Enceladus and Titan revealed a wealth of chemical complexity of neutral and positively  
224 charged molecules. However, analysis was restricted by mass spectroscopic instruments, which  
225 were limited by their low sensitivity, mass range, and resolution and subsequent inability to resolve  
226 high-mass isobaric molecular species, neutral and positive ions. For example, in Enceladus' vapor  
227 plume an unidentified species with a mass-to-charge ( $m/z$ ) ratio of 28, which is thought to be either  
228 CO, N<sub>2</sub>, C<sub>2</sub>H<sub>4</sub> or a combination of these compounds was detected. Determining the abundance  
229 ratio between these different species is essential to constrain the origin of volatiles on Enceladus  
230 and to assess whether they were reprocessed internally. The evidence of high temperature  
231 hydrothermal activity (Hsu et al. 2015) within Enceladus' subsurface ocean provides strong  
232 incentive to test the plume for prebiotic and biotic signatures using high-resolution spectrometers.  
233 Further, putative exothermic water-rock interactions on Enceladus could be further constrained by  
234 quantifying H<sub>2</sub> in the plume. On Titan, higher resolution spectroscopic instruments would enable  
235 better constraints on complex organic processes and components occurring in Titan's atmosphere,  
236 particularly those with prebiotic and biotic potential.

237

238 The geology and morphology of both Titan and Enceladus has been revealed by Cassini Visual  
239 and Infrared Mapping spectrometer (VIMS), Imaging Science Subsystem (ISS) and RADAR SAR  
240 imagery but only at low to moderate resolutions. Additionally, imaging of the surface was also  
241 constrained on Titan by scattering of atmospheric aerosols and absorption that limited SNR. A  
242 future mission to Titan can provide images in the mid-IR range at or around 5  $\mu\text{m}$  since images at  
243 these wavelengths are subject to minimal scattering (Soderblom et al. 2012; Barnes et al. 2013)  
244 enabling diffraction limited images that are extremely sensitive to composition (Clark et al. 2010;  
245 Barnes et al. 2014) with spatial resolutions an order of magnitude better than Cassini observations  
246 (Clark et al. 2010; Soderblom et al. 2012; Barnes et al. 2014). A high-resolution map would enable  
247 a vastly improved investigation of Titan's geology, hydrology, and compositional variability and  
248 would enable the detection of morphology not evident from Cassini data, quantify geological  
249 processes and relationships between different geological units and examine alterations due to  
250 geologic, atmospheric or seasonal activity. Recently an ice-rich linear feature of bedrock, covering  
251 40% of Titan's circumference was discovered using statistical analysis of 13,000 Cassini VIMS  
252 images (Griffith et al. 2019); it is likely many features with weaker spectral signatures remain to  
253 be discovered. High-resolution imaging of Enceladus' SPT will provide new detail of the  
254 tectonically active surface, constrain characteristics of the hydrothermal system by investigating  
255 the composition and kinematics of Enceladus' jets and plumes. Further IR imaging will view  
256 thermal emission from Enceladus' hot spots and constrain the presence of anomalous heat  
257 signatures in the SPT (Le Gall et al. 2017) at resolutions comparable to ISS observations of the  
258 SPT.

259

260

TABLE 1

261  
262  
263  
264  
265  
266  
267  
268  
269  
270  
271  
272  
273  
274  
275  
276  
277  
278  
279  
280  
281  
282  
283

TABLE 2  
TABLE 3

Gravity field measurements are powerful tools to constrain the interior structure and to assess mass anomalies, providing information on the internal dynamics and evolution. Gravity measurements of Enceladus' south pole can be used to find a local solution of the SPT gravity field and its time-variation (using along-track data) rather than a global solution. In the south polar region, we expect a larger time-variation of the gravity field with respect to the global solution of the time variation of the gravity field due to the fact that the ice shell thickness is expected to be locally thin at the SPT. A radio science experiment that will determine the local solution of the gravity field of Enceladus at the SPT will allow the determination of the thickness variation at the south polar regions and constraints on the mechanical properties (viscosity) of the ice overlying an outer ice shell. The expected tidal deformation is characterized by a pattern more complex than the standard degree-two pattern, with a strong amplification of the tidal fluctuation in the SPT (Brzobohaty et al. 2016). Should a final Titan orbiter phase be included in the baseline mission, higher degrees of gravity coefficients, up to at least degrees twelve could be obtained as well as an estimation of the real and imaginary parts of Titan's  $k_2$  with an accuracy of 0.0001 (Tortora et al. 2017). The characterization of the global gravity field of Titan and/or Enceladus might also be significantly improved through a pair of companion small satellites, to be released by the mothership around either moons. This element may complement the science observations of the larger spacecraft, through a combination of Satellite-to-Satellite Tracking (SST) between two smallsats or between one smallsat and the mothership. Preliminary simulations have shown that in just three months this technique would allow to estimate the static gravity field up to at least degree thirteen (for Titan)

284 and degree twenty (for Enceladus), while the real and imaginary part of  $k_2$  can reach an accuracy  
285 of about 0.08 for Titan and 0.002 for Enceladus (Tortora et al. 2018a, Tortora et al. 2018b). This  
286 optional element may be studied in parallel to the more consolidated Options a) and b) listed above.  
287 The subsurface processes and structures of both Titan and Enceladus can be further investigated  
288 with an ice penetrating radar (IPR), which uses microwaves to penetrate through the surface to  
289 examine subsurface characteristics. Structural, thermal and compositional profiles of subsurface  
290 structures and thickness of the regolith layer can be used to characterize the surface and subsurface  
291 structures and determine their correlation to each other. Further determination of the ice-ocean  
292 interface at Enceladus' SPT and the brittle-ductile interface within Titan's ice shell can constrain  
293 evolutionary and thermal processes. Radar sounding instruments have been used in multiple space  
294 missions on Mars and the Moon (e.g., Heggy et al. 2006; Seu et al. 2007; Picardi et al. 2004; Ono  
295 et al. 2010) and will be used to examine Europa and Ganymede in the Jupiter system in ESA's  
296 upcoming JUICE mission (Bruzzone et al. 2013, 2015). The upcoming NASA mission, Europa  
297 Clipper, will radar sound Europa during a series of multiple flybys while in orbit around Jupiter  
298 (Blankenship et al. 2009).

299  
300 While Cassini has provided stunning imagery of Titan's lakes and seas (e.g. Stofan et al. 2007)  
301 and VIMS and RADAR data have been used to constrain their composition and bathymetry  
302 (Brown et al. 2008; Mastrogiuseppe et al., 2014; Lopes et al., 2019), open questions regarding  
303 their formation, particularly smaller sharp edge depression lakes, the extant of subsurface  
304 communication, composition of the lakes and seas and the evaporites that often surround them as  
305 well as paleolakes in the south pole and possible presence of lakes or empty lake basins outside  
306 the polar regions still remain (e.g. Nixon et al. 2018). The combination of high resolution remote

307 sensing and *in situ* measurements can answer many questions. In addition, *in situ* studies of one of  
308 Titan’s seas would complement data obtained by the Dragonfly mission, which was recently  
309 selected by NASA as part of its New Frontiers program as an upcoming mission to be launched in  
310 2026 and arrive at Titan in 2034. The Dragonfly mission while unprecedented is only regional in  
311 scope exploring the low-latitude Selk impact crater region with a flying rotorcraft drone. Thus *in*  
312 *situ* exploration of a northern sea and global observations of Titan are important science goals that  
313 remain to be addressed by a future mission to the Saturn system.

314

315 Science goals to be resolved by a future baseline multiple flyby mission to Titan and Enceladus,  
316 based on the E<sup>2</sup>T mission proposed for ESA M5 study (Mitri et al. 2018) are shown in Table 1.  
317 Additional science goals that can be investigated with the option #1 of *in situ* exploration of a  
318 northern sea and/or the option #2 of radar sounding of the surface of Titan and Enceladus SPT  
319 during multiple flybys or Titan’s orbiter are described in Table 2 and Table 3 respectively.

320

### 321 **3. Missions scenarios**

#### 322 **3.1 Baseline mission scenario**

323 The proposed baseline mission concept consists of a solar-electric powered spacecraft performing  
324 multiple flybys of Titan and Enceladus while in orbit around Saturn. The proposed baseline  
325 mission is based on the Explorer of Enceladus and Titan (E<sup>2</sup>T) proposed as a medium-class mission  
326 led by ESA in collaboration with NASA in response to ESA’s M5 Call (Mitri et al. 2018). The  
327 proposed baseline mission concept for this White Paper is for a large class ESA mission (class L).  
328 The evaluated cost from ESA review for E<sup>2</sup>T is 950 M€ that fit in a large mission budget constraint.

329

330

FIGURE 3

331

332 The baseline payload would consist of three scientific instruments: two time-of-flight mass  
333 spectrometers and a high-resolution infrared camera, while the telecommunication system would  
334 be utilized to perform gravity science. The baseline interplanetary transfer, cruise and flyby phases  
335 are all based on a proposed launch in 2029–2030 and therefore are included only as example  
336 trajectories. After the launch, the S/C will transfer from geosynchronous transfer orbit (GTO) to a  
337 hyperbolic escape trajectory and would pursue a gravity assist flyby of the Earth to help propel  
338 itself to the Saturn system. The cruise phase from Earth to Saturn would be 6 years long. After the  
339 arrival in the Saturn system, the mission is divided in a first Enceladus science phase and in a  
340 second Titan science phase. The S/C should perform at least 6 flybys of Enceladus above the south  
341 polar terrain (SPT) and at least 17 flybys of Titan. To prevent contamination of Enceladus science  
342 by Titan’s organics, E<sup>2</sup>T S/C will perform close flybys of Enceladus at the beginning of the tour  
343 (Enceladus science phase); distant flybys of Titan will be performed during the initial tour phase.

344

345

FIGURE 4

346

347 After the main Enceladus phase, close flybys of Titan with atmospheric sampling will be  
348 performed (Titan science phase). During the Titan science phase, the S/C will provide *in situ*  
349 sampling of the upper atmosphere at a minimum altitude from Titan surface as low as 900 km  
350 using mass spectrometers. At the closest approach the velocity of the S/C with respect to Titan’s  
351 surface will be ~7 km/s. Imaging data would be collected during inbound and outbound segments  
352 of each flyby. The duration of the tour from its arrival in the Saturn system to the end of the 17-



353 flyby Titan phase is about 3.5 years. Figure 3 shows a proposed interplanetary transfer to Saturn  
354 and Figure 4 shows a proposed sample tour. Both Figures 3 and 4 are based on a proposed E<sup>2</sup>T  
355 launch of 2029–2030 (Mitri et al. 2018). Figure 5 shows the proposed configuration of the S/C for  
356 the E<sup>2</sup>T project. While the baseline mission is conceived as a multiply flyby mission it can also  
357 include a final orbiter phase around Titan similar to the final orbiter phase of the JUICE (JUperiter  
358 ICy moons Explorer) spacecraft around Ganymede in the upcoming ESA JUICE mission.

359

### 360 **3.2 Option 1: Titan sea lander**

361 The S/C will carry a scientific payload consisting of remote sensing instruments and experiments  
362 aforementioned while if Option #1 is utilized the S/C will also carry an Entry, Descent and Landing  
363 (EDL) module containing a sea lander equipped with an instrument suite capable of carrying out  
364 *in situ* measurements of one of Titan’s north polar seas. Figure 6 shows a proposed sea lander and  
365 entry vehicle. During the descent, the probe will make *in situ* measurement of the atmosphere.  
366 Once a successful splashdown has been achieved, the sea probe will be taking measurements  
367 sampling both the liquid of the seas and the atmosphere above. Previous analysis for a mission that  
368 considered the exploration of Titan using an orbiter, a lake-probe and a balloon demonstrated the  
369 feasibility of such mission (the Titan Saturn System Mission Study TSSM, Coustenis et al. 2009)  
370 as did the study of the Titan Mare Explorer (TiME) (Stofan et al. 2010) which was a lake lander  
371 only mission to *in-situ* investigate one of the large north polar mare on Titan. In addition, Mitri et  
372 al. (2014a) presented the science case for the exploration of Titan and one of its seas with an orbiter  
373 and a lake probe. If Option #2 is utilized, the S/C will carry a nadir-looking ice penetrating radar  
374 sounder (IPR).

375

376 The sea lander will sample Titan's atmosphere obtaining temperature, wind, humidity and  
377 composition profiles during its descent. Once the sea lander is in the Titan sea, it will make a  
378 number of measurements including bulk and trace composition of the sea and lower atmosphere,  
379 and bathymetric and shoreline profiles; additionally, the shoreline of the sea can be imaged during  
380 the descent. Possible instrument suite utilized by a sea lander with associated science goals and  
381 measurements is shown in Table 4 (Mitri et al. 2014a).

382

383 The sea lander will relay data to the S/C, which will serve as the communications link between the  
384 probe and Earth. Direct-to-Earth (DTE) communication of the sea lander is a possible  
385 complementary communication method. Lorenz and Newman (2015) have found that the seasonal  
386 geometry at Titan's north pole allows DTE from the seas until 2026 and after 2040. Given the  
387 opacity of Titan's atmosphere, the use of a solar powered generator for the sea-probe is infeasible  
388 if its operations need to last more than a few hours. The sea lander portion of the proposed mission  
389 will be short-lived due to technical constraints. Current technology dictates that the use of batteries  
390 will only provide power to the sea lander on the order of hours; though this technology will likely  
391 improve. The sea lander will not have propulsion capabilities rather it will be propelled around the  
392 lake by winds and possible tides; Lorenz and Mann (2015) have studied the wind and wave  
393 conditions that a floating Titan sea lander might encounter. Testing of a scale model of the  
394 proposed Titan Mare Explorer sea lander capsule has revealed important data regarding potential  
395 science operations and lander-lake dynamics (Lorenz et al. 2015; Lorenz and Cabrol 2015). Recent  
396 work proposes that a sea-lander could possibly not only float but also be able to propel itself

397 utilizing mechanical tensegrity structures (Gebara et al. 2019). The use of a radioisotopic power  
398 generator for the sea probe could be requested using technology, which could significantly reduce  
399 the amount of plutonium fuel. The Advanced Stirling Radioisotopic Generator (ASRG), based on  
400 Stirling power conversion technology, offers a four-fold reduction in the amount of plutonium fuel  
401 compared to radioisotope thermal generators (RTG) used in previous interplanetary missions  
402 (Stofan et al. 2010); while NASA has ended funding for in-flight development of ASRG  
403 technology in 2013 due to budget cuts, research continues on this technology and other  
404 radioisotope power systems in NASA (Oriti and Schmitz 2019). Additionally, the development of  
405 radioisotopic power using Americium ( $^{241}\text{Am}$ ) currently being developed by ESA since 2008 is  
406 another possible option (Barco et al. 2019).

407

408

FIGURE 6

409

TABLE 4

410

### 411 **3.3 Option 2: Radar sounder**

412 The ice penetrating radar, following the heritage of JUICE RIME and Europa Clipper REASON,  
413 would be capable of both shallow and deep sounding to characterize the subsurface with a depth  
414 of 9 km and ~30 m vertical resolution at minimum. Both RIME and REASON are to operate at a  
415 HF band with a center-frequency of 9 MHz and possess bandwidths between 1 and 3 MHz while  
416 REASON operates at an additional VHF frequency with a center frequency of 60 MHz (Bruzzone  
417 et al. 2013; Grima et al. 2015). An IPR can characterize structural, compositional and thermal  
418 variations occurring in the subsurface providing data that can correlate surface and subsurface

419 features and processes, deformation in the upper ice shell, as well as global and local surface age.  
420 In addition, an IPR can also investigate the ice-ocean interface at Enceladus' SPT and brittle-  
421 ductile transition on Titan constraining the thickness and thermal evolution of the ice shells. An  
422 additional option for radar architecture could be a multi-mode radar design suitable for both  
423 sounding and imaging to be operated in two modes: a vertical sounder mode with similar  
424 capabilities as described above though with different architecture, and a Synthetic Aperture Radar  
425 (SAR) imaging mode, similar to Cassini (Elachi et al., 2004), but with a higher resolution at tens  
426 of meters. The additional SAR mode could be used for high-resolution imaging of the surface,  
427 complementing the IR imaging, as well as for creating three-dimensional high-resolution  
428 bathymetric maps of Titan seas and lakes and could permit investigation of any possible  
429 compositional variation in space and time of the hydrocarbon liquid and/or sea floor properties.

430

#### 431 **4. Science case for the baseline mission scenario**

432 In this section we discuss the science goals and themes for the proposed baseline mission based  
433 on the E<sup>2</sup>T mission submitted to ESA in response to the M5 Call (Mitri et al. 2018). Discussion of  
434 the science themes of the proposed mission options is discussed in Section 5.

435

#### 436 **4.1 Origin and evolution of volatile-rich ocean worlds, Enceladus and Titan**

437 The origin of volatiles currently present on Titan and Enceladus is still being debated. New data  
438 are needed to determine if the volatile inventory is primordial, originating in the solar nebula or

439 Saturnian subnebula possibly altered during the accretion process or else were produced in some  
440 secondary manner is still being debated (e.g., Atreya et al. 2006). How photochemical processes  
441 on Titan and aqueous alteration on Enceladus have affected the initial volatile inventory remains  
442 unknown. Given that a late accretion scenario may explain the mass distribution and ice/rock ratio  
443 of the mid-sized moons in the Saturn system, Enceladus may have formed less than 1 billion years  
444 ago, while Titan may have accreted early. This may have resulted in significant differences in their  
445 initial volatile inventory and their subsequent evolution.

446

447 By combining *in situ* chemical analysis of Titan's atmosphere and Enceladus' plume with  
448 observations of Enceladus' plume dynamics and Titan's surface geology, a future mission can  
449 provide constraints on how these ocean worlds acquired their initial volatile inventory and how it  
450 was subsequently modified during their evolution (Lunine et al. 2018); these investigations can  
451 improve our understanding of the nature of Saturn subnebula formation conditions and its  
452 subsequent evolution as well as the conditions of the early solar nebula, the nature of cometary  
453 and giant impacts, all of which might also help to predict the physical and chemical properties of  
454 terrestrial planets and exoplanets beyond the Solar System.

455

#### 456 **4.2 Chemical constraints on the origin and evolution of Titan and Enceladus**

457 The origin and evolution of Titan's methane still needs to be constrained. Whether Titan's methane  
458 is primordial likely through water-rock interactions in Titan's interior during its accretionary phase  
459 (Atreya et al. 2006) or else delivered to Titan during its formation processes (Mousis et al. 2009)

460 or by cometary impacts (Zahnle et al. 1992; Griffith and Zahnle 1995) is a key open question. On  
461 Titan, the Huygens probe detected small argon abundance ( $^{36}\text{Ar}$ ) and a tentative amount of neon  
462 ( $^{22}\text{Ne}$ ) in its atmosphere (Niemann et al. 2005, 2010), but was unable to detect the corresponding  
463 abundance of xenon and krypton. The presence of  $^{22}\text{Ne}$  ( $^{36}\text{Ar}/^{22}\text{Ne}\sim 1$ ) was unexpected as neon is  
464 not expected to be present in any significant amounts in protosolar ices (Niemann et al. 2005,  
465 2010) and may indicate water-rock interactions and outgassing processes (Tobie et al. 2012). The  
466 non-detection of xenon and krypton supports the idea that Titan's methane was generated by  
467 serpentinization of primordial carbon monoxide and carbon dioxide delivered by volatile depleted  
468 planetesimals originating from within Saturn's subnebula (e.g., Atreya et al. 2006). Xenon and  
469 krypton would both have to be sequestered from the atmosphere to support a primordial methane  
470 source. While xenon is soluble in liquid hydrocarbons (solubility of  $10^{-3}$  at 95 K) and could  
471 potentially be sequestered into liquid reservoirs, argon and krypton cannot (Cordier et al. 2010).  
472 Therefore, the absence of measurable atmospheric krypton requires either sequestration into non-  
473 liquid surface deposits, such as clathrates (Mousis et al. 2011), or depletion in the noble gas  
474 concentration of the planetesimals (Owen and Niemann 2009). Unlike Cassini INMS, which was  
475 developed in the 1990s, current and future spectrometers have the mass range and sensitivity to  
476 accurately measure xenon. Measurement of the abundance of noble gases in the upper atmosphere  
477 of Titan can discriminate between crustal carbon sequestration and carbon delivery via depleted  
478 planetesimals.

479

480 The longevity of methane in Titan's atmosphere is still a mystery. The value of  $^{12}\text{C}/^{13}\text{C}$  in Titan's  
481 atmosphere has been used to conclude that methane outgassed  $\sim 10^7$  years ago (Yung et al. 1984)

482 and is being lost via photolysis and atmospheric escape (Yelle et al. 2008). It is an open question  
483 whether the current methane rich atmosphere is a unique event, whether it is in a steady state where  
484 methane destruction and replenishment are in balance (Jennings et al. 2009), or else is a unique  
485 transient event and is in a non-steady state where methane is being actively depleted or replenished.  
486 Indeed, the possibility that Titan did not always possess a methane rich atmosphere seems to be  
487 supported by the fact that the amount of ethane on Titan's surface should be larger than the present  
488 inventory (this is further discussed in the geological processes section below); though Wilson and  
489 Atreya (2009) contend that missing surface deposits may simply be reburied into Titan's crust and  
490 Mousis and Schmitt (2008) have shown that it is possible for liquid ethane to react with a water-  
491 ice and methane-clathrate crust to create ethane clathrates and release methane. Nixon et al. (2012),  
492 however, favor a model in which methane is not being replenished and suggest atmospheric  
493 methane duration is likely between 300 and 600 Ma given that Hörst et al. (2008) demonstrated  
494 that 300 Ma is necessary to create Titan's current CO inventory and recent surface age estimates  
495 based on cratering (Neish and Lorenz 2012). Mandt et al. (2012) suggests that methane's presence  
496 in the atmosphere, assumed here to be due to outgassing, has an upper limit of 470 Ma or else up  
497 to 940 Ma if the presumed methane outgassing rate was large enough to overcome  $^{12}\text{C}/^{13}\text{C}$  isotope  
498 fractionation resulting from photochemistry and escape. Both the results of Mandt et al. (2012)  
499 and Nixon et al. (2012) fall into the timeline suggested by interior models (Tobie et al. 2006) which  
500 suggests that the methane atmosphere is the result of an outgassing episode that occurred between  
501 350 and 1350 Ma.

502

503

FIGURE 7

504

505 On Titan, both simple (methane, ethane and propane) and complex hydrocarbons precipitate out  
506 of the atmosphere and onto the surface. Measuring the isotopic ratios ( $^{14}\text{N}/^{15}\text{N}$ ;  $^{12}\text{C}/^{13}\text{C}$ ; D/H;  
507  $^{16}\text{O}/^{18}\text{O}$ ) and abundances of the simple alkanes (e.g., methane, ethane and propane) will constrain  
508 the formation and evolution of the methane cycle on Titan. Further measurements of radiogenic  
509 noble gases such as  $^{40}\text{Ar}$  and  $^{22}\text{Ne}$ , which are typically markers of volatile elements from Titan's  
510 interior can constrain outgassing episodes. Detection of  $^{40}\text{Ar}$  and tentatively  $^{22}\text{Ne}$  in the atmosphere  
511 has provided circumstantial evidence of water-rock interactions and methane outgassing from the  
512 interior (Niemann et al. 2010; Tobie et al. 2012). Measurements of the composition and isotopic  
513 ratios of Titan's upper atmosphere in a future mission can be used to determine the age of methane  
514 in the atmosphere and characterize outgassing history.

515

516 On Enceladus, Cassini measurements by INMS (Waite et al. 2006, 2009) and UVIS (Hansen et al.  
517 2006, 2008) showed that plume gas consists primarily of water vapor with a few percent other  
518 volatiles (Figure 7). In addition to  $\text{H}_2\text{O}$  as the dominant species, INMS was able to identify  $\text{CO}_2$   
519 ( $0.6\% \pm 0.15\%$ ),  $\text{CH}_4$  ( $0.23\% \pm 0.06\%$ ), and  $\text{NH}_3$  ( $0.7\% \pm 0.2\%$ ) in the vapor plume as well as an  
520 unidentified species with a mass-to-charge ( $m/z$ ) ratio of 28, which is thought to be either  $\text{CO}$ ,  $\text{N}_2$ ,  
521  $\text{C}_2\text{H}_4$  or a combination of these compounds. The low mass resolution of Cassini INMS is  
522 insufficient to separate these species, and the UVIS measurements can only provide upper limits  
523 on  $\text{N}_2$  and  $\text{CO}$  abundance. Determining the abundance ratio between these different species is,  
524 however, essential to constrain the origin of volatiles on Enceladus and to assess whether they  
525 were reprocessed internally. A high  $\text{CO}/\text{N}_2$  ratio, for instance, would suggest a cometary-like



526 source with only a moderate modification of the volatile inventory, whereas a low CO/N<sub>2</sub> ratio  
527 would indicate a significant internal reprocessing.

528

529 In addition to these main volatile species, during some Cassini flybys, the INMS data also indicated  
530 the possible presence of trace quantities of C<sub>2</sub>H<sub>2</sub>, C<sub>3</sub>H<sub>8</sub>, C<sub>4</sub>, methanol, formaldehyde and hydrogen  
531 sulfide. Organic species above the INMS mass range of 99 u are also present but could not be  
532 further constrained (Waite et al. 2009). The identification and the quantification of the abundances  
533 of these trace species remains very uncertain due to the limitations of the mass spectrometer on  
534 board Cassini.

535

536 Except for the measurement of D/H in H<sub>2</sub>O on Enceladus (which has large uncertainty, Waite et  
537 al. 2009), no information is yet available for the isotopic ratio in Enceladus' plume gas. The  
538 baseline mission would determine the isotopic ratios (D/H, <sup>12</sup>C/<sup>13</sup>C, <sup>16</sup>O/<sup>18</sup>O, <sup>14</sup>N/<sup>15</sup>N) in major gas  
539 compounds of Enceladus' plume as well as <sup>12</sup>C/<sup>13</sup>C in organics contained in icy grains. Comparison  
540 of gas isotopic ratios (e.g., D/H in H<sub>2</sub>O and CH<sub>4</sub>, <sup>12</sup>C/<sup>13</sup>C in CH<sub>4</sub>, CO<sub>2</sub>, and CO; <sup>16</sup>O/<sup>18</sup>O in H<sub>2</sub>O,  
541 CO<sub>2</sub>, CO; <sup>14</sup>N/<sup>15</sup>N in NH<sub>3</sub> and N<sub>2</sub>) and with Solar System standards will provide essential  
542 constraints on the origin of volatiles and how they may have been internally reprocessed.  
543 Simultaneous precise determination of isotopic ratios in N, H, C and O-bearing species in  
544 Enceladus' plume and Titan's atmosphere will permit a better determination of the initial reference  
545 values and a quantification of the fractionation due to internal and atmospheric processes on both  
546 moons.

547

548 Noble gases also provide essential information on how volatiles were delivered to Enceladus and  
549 whether significant exchanges between the rock phase and water-ice phase occurred during  
550 Enceladus' evolution. The detection and quantification of  $^{36}\text{Ar}$  and  $^{38}\text{Ar}$  will place fundamental  
551 constraints on the volatile delivery in the Saturn system. A low  $^{36}\text{Ar}/\text{N}_2$  ratio, for instance, would  
552 indicate that  $\text{N}_2$  on Enceladus is not primordial, like on Titan (Niemann et al. 2010), and that the  
553 fraction of argon brought by cometary materials on Enceladus is rather low. In addition to argon,  
554 if Ne, Kr, and Xe are present in detectable amounts, the baseline mission would be able to test  
555 whether primordial noble gases on Enceladus were primarily brought by a chondritic phase or  
556 cometary ice phase, which has implications for all the other primordial volatiles. The  
557  $^{40}\text{Ar}/^{38}\text{Ar}/^{36}\text{Ar}$  as well as  $^{20}\text{N}/^{21}\text{Ne}/^{22}\text{Ne}$  measured ratios will also allow for testing of how noble  
558 gases were extracted from the rocky core. Abundance ratios between  $\text{Ar}/\text{Kr}$  and  $\text{Ar}/\text{Xe}$ , if Kr and  
559 Xe are above detection limit, will offer an opportunity to test the influence of clathration storage  
560 and decomposition in volatile exchanges through Enceladus's ice shell.

561

562 The origin of methane detected in Enceladus' plume is still uncertain. Methane, ubiquitous in the  
563 interstellar medium was most likely embedded in the protosolar nebula gas. The inflow of  
564 protosolar nebular gas into the Saturn subnebula may have trapped methane in clathrates that were  
565 embedded in the planetesimals of Enceladus during their formation. Alternatively, methane may  
566 have been produced via hydrothermal reactions in Enceladus' interior. Mousis et al. (2009)  
567 suggests that if the methane of Enceladus originates from the solar nebula, then  $\text{Xe}/\text{H}_2\text{O}$  and  
568  $\text{Kr}/\text{H}_2\text{O}$  ratios are predicted to be equal to  $\sim 7 \times 10^{-7}$  and  $7 \times 10^{-6}$  in the satellite's interior,

569 respectively. On the other hand, if the methane of Enceladus results from hydrothermal reactions,  
570 then Kr/H<sub>2</sub>O should not exceed  $\sim 10^{-10}$  and Xe/H<sub>2</sub>O should range between  $\sim 1 \times 10^{-7}$  and  $7 \times 10^{-7}$  in  
571 the satellite's interior.

572

### 573 **4.3 Compositional variability in Enceladus' plume**

574 The detection of salty ice grains (Postberg et al. 2009, 2011), the high solid-to-vapor ratio (Porco  
575 et al. 2006; Ingersoll and Ewald, 2011), and the observations of large particles in the lower part of  
576 the plume (Hedman et al. 2009) all indicate that the plume of Enceladus originates from a liquid  
577 source likely from the subsurface ocean rather than from active melting within the outer ice shell.  
578 However, the abundance of the major gas species observed by Cassini suggests some contribution  
579 from the surrounding cold icy crust should also be considered. Cassini observations show that the  
580 plume is made up of  $\sim 100$  discrete collimated jets as well as a broad, diffuse component (Hansen  
581 et al. 2008, 2011; Postberg et al. 2011; Porco et al. 2014). The majority of plume material is found  
582 in the distributed diffuse portion of the plume while only a small portion of gas and grains are  
583 emitted from the jets (Hansen et al. 2011; Postberg et al. 2011). The saltiness of the ice grains and  
584 recent detection of nanometer sized silica dust particles in E-ring stream particles (Hsu et al. 2011,  
585 2015) all indicate their origin is a location where alkaline high temperature hydrothermal reactions  
586 and likely water-rock interactions are occurring.

587

588 Although the Cassini (Cosmic Dust Analyzer) CDA has constrained knowledge of plume  
589 compositional stratigraphy, measurements of the absolute abundance and composition of organics,

590 silicates and salts are poorly constrained given the low spatial resolution (10 km), low mass  
591 resolution and limited mass range of the CDA. The Cassini INMS provided only plume integrated  
592 spectra and is not able to separate gas species with the same nominal mass. However, current high  
593 mass resolution, spectrometers have a resolution that is 50 times larger than that of Cassini INMS,  
594 and would allow for the separation of isobaric interferences, for example separating  $^{13}\text{C}$  and  $^{12}\text{CH}$   
595 and  $\text{CO}$  and  $\text{N}_2$ . Determining high-resolution spatial variations in composition is crucial to  
596 establish whether the jets are fed by a common liquid reservoir or if jet sources are disconnected,  
597 and if the local liquid sources interact with a heterogeneous in the icy shell. Variations in  
598 composition between the solid and gas phases as a function of distance from jet sources can also  
599 provide information about how the less volatile species condense on the grains, thus constraining  
600 the eruption mechanisms.

601

#### 602 **4.4 Geological constraints on Titan's methane cycle and surface evolution**

603 As discussed above, there is an open question on whether Titan's methane-rich atmosphere is being  
604 actively replenished, or if methane is being lost and Titan's methane may eventually be depleted  
605 (Yung et al. 1984). Cryovolcanism has been suggested as a mechanism by which methane and  
606 argon can be transported from Titan's interior to its surface (e.g., Lopes et al. 2013). Cryovolcanic  
607 activity may also promote methane outgassing (Tobie et al. 2006); while methane clathrates are  
608 stable in Titan's ice shell in the absence of destabilizing thermal perturbations and/or pressure  
609 variation, variations in the thermal structure of Titan's outer ice shell during its evolution could  
610 have produced thermal destabilization of methane clathrates generating outgassing events from the  
611 interior to the atmosphere (Tobie et al. 2006; see also Davies et al. 2016). A number of candidate

612 cryovolcanic features have been identified in Cassini observations (Lopes et al. 2013). High-  
613 resolution color images from the proposed baseline mission would provide the data needed to  
614 determine the geneses of these features. Stratigraphic relationships and crater counting will provide  
615 a means by which the relative ages of these features may be constrained.

616

617 A related question to the age of Titan's atmosphere is whether Titan's climate is changing. At  
618 present, most of the observed liquid methane is located in the north polar region (Aharonson et al.  
619 2009). There have been suggestions, however, that organic seas may have existed in Titan's tropics  
620 (Moore and Howard 2010; MacKenzie et al. 2014), and/or in broad depressions in the south  
621 (Aharonson et al. 2009; Hayes et al. 2011). Models suggest Titan's methane distribution varies on  
622 seasonal timescales (e.g., Hayes et al. 2010; Turtle et al. 2011) or Milankovitch timescales  
623 (Aharonson et al. 2009). Alternative models suggest that methane is being depleted and Titan's  
624 atmosphere is drying out (Moore and Howard 2010). High-resolution images of the margins and  
625 interiors of these basins will allow us to determine whether they once held seas. Identification of  
626 impact features or aeolian processes within these basins will help to constrain the timing of their  
627 desiccation.

628

629 In addition to their inherent scientific interest, Titan's dunes also serve as a witness plate to climatic  
630 evolution. Larger dune forms take longer to form than smaller dune forms. In Earth's Namib desert,  
631 these differing timescales result in large, longitudinal dunes that adhere to the overall wind  
632 conditions from the Pleistocene 20,000 years ago, while smaller superposing dunes (sometimes

633 called rake dunes, or flanking dunes) have responded to the winds during our current interglacial  
634 and orient ages accordingly. On Titan, a high-resolution infrared camera could resolve these  
635 potential smaller dunes on top of the known longitudinal dunes and will therefore reveal if Titan's  
636 recent climate has been stable or if it has changed over the past few Ma. Titan's geology is unique  
637 in that liquid and solid organics likely play key roles in many of the observed processes. As these  
638 processes play an important role in the modification of organics on Titan, both physically and  
639 chemically, understanding them is crucial for determining the complex chemistry that likely occurs  
640 on this moon. Furthermore, study of Titan's geology allows us to investigate processes that are  
641 also common on Earth, but in drastically different environmental conditions, providing a unique  
642 way to gain insight into the processes that shaped the Earth and pre-Noachian Mars.

643

644 Observations of Titan suggest the landscape is significantly modified by liquid organics (e.g., Burr  
645 et al. 2013). Fluvial erosion is observed at all latitudes, with a variety of morphologies suggesting  
646 a range of controls and fluvial processes (Burr et al. 2013). High-resolution color imaging will  
647 provide insight into the nature of this erosion: whether it is predominantly pluvial or sapping in  
648 nature and whether it is dominated by mechanical erosion or dissolution. Dissolution processes are  
649 suspected to control the landscape of Titan's labyrinth terrains (Cornet et al. 2015) and may also  
650 be responsible for the formation of the polar sharp-edged depressions (Hayes et al. 2008), though  
651 a new model suggests that the sharp-edged depressions with raised rims may be craters formed by  
652 explosions of subsurface pressurized nitrogen during colder methane-depleted periods in Titan's  
653 past (Mitri et al., 2019). High-resolution imaging will allow direct testing of these hypotheses in  
654 the proposed baseline mission.

655

656 Both fluvial and aeolian processes likely produce and transport sediments on Titan. Dunes are  
657 observed across Titan's equator (Radebaugh et al. 2008; Malaska et al. 2016) while a variety of  
658 fluvial sediment deposits can be identified in SAR data (Burr et al. 2013; Birch et al. 2016).  
659 Detailed imagery of the margins of the dune fields will allow us to determine the source and fate  
660 of sands on Titan. High-resolution images will also help determine whether the observed fluvial  
661 features are river valleys or channels (cf. Burr et al. 2013) providing key information in obtaining  
662 accurate discharge estimates needed to model sediment transport (Burr et al. 2006) as well as  
663 provide insight into the primary erosion processes acting on crater rims, which are likely composed  
664 of a mixture of organics and water ice (Soderblom et al., 2007; Neish et al. 2015, 2016). Finally,  
665 improved imaging will provide insight into the nature of erosion that exists in Titan's mid-  
666 latitudes, a region that shows little variability in Cassini observations.

667

668 Of great interest in understanding the evolution of Titan's surface is determining the nature of the  
669 observed geologic units, including their mechanical and chemical properties. Fluvial processes,  
670 the degree to which mechanical vs dissolution dominates and the existence of sapping, reflect the  
671 material properties of the surface and therefore can be used as a powerful tool to investigate the  
672 properties of the surface. The baseline mission imaging would also allow us to investigate the  
673 strength of the surface materials by constraining the maximum slopes supported by different  
674 geologic units. High-resolution detailed color and stereo imaging of the boundaries of units will  
675 also allow investigation of the morphology, topography, and spectral relationship across unit  
676 boundaries.

677

678 **4.5 Habitability and potential for life in ocean worlds, Enceladus and Titan**

679 Ocean worlds, such as Titan and Enceladus, are objects of wide astrobiological interest because  
680 water is one of the key prerequisites for life, in addition to nutrients and energy. Additionally, the  
681 organic surface environment of Titan provides an ideal, and in many ways unique setting to  
682 investigate the prebiotic chemistry that may have led to the emergence of life on the Earth. Water  
683 on ocean worlds in the outer Solar System is found underneath the surface of insulating ice shells,  
684 which regulate heat and chemical transport.

685

686 The dissipation of energy from tidal flexing, combined with radiogenic energy from these moons’  
687 interior provide the energy to sustain these oceans. The presence of antifreeze elements, such as  
688 salts or ammonia, suggested by mass spectrometric measurements on Titan and Enceladus  
689 (Niemann et al. 2005; Waite et al. 2009) and accretion models (Lunine and Stevenson 1987;  
690 Mousis et al. 2002) may also play an important role in sustaining these subsurface oceans.  
691 Subsurface oceans are known to exist on both Titan and Enceladus based on Cassini-Huygens  
692 mission gravity, shape and libration data (Iess et al. 2010, 2012, 2014; Mitri et al. 2014b;  
693 McKinnon 2015; Thomas et al. 2016), compositional *in situ* measurements and thermal evolution  
694 models (Tobie et al. 2005, 2006; Mitri and Showman 2008). Enceladus is unique in that  
695 communication of this water is known to exist between the surface and the subsurface and, quite  
696 conveniently, this water is ejected into space for easy *in situ* sampling. Titan provides its own  
697 unique environment in which a rich array of complex organics exists on the surface and may



698 interact with the subsurface ocean via cryovolcanic activity or, alternatively, with transient liquid  
699 water at the surface following impact events.

700

701 Because the presence of a subsurface ocean decouples the interior from the outer ice shell, there is  
702 a much larger ice shell deflection and thus enhanced tidal heating and stresses in the shell; therefore  
703 tectonic features are much more likely on ocean worlds (Mitri et al. 2010; Nimmo and Pappalardo  
704 2016) than on icy satellites without subsurface oceans. Surface geological activity may also lead  
705 to transport of surface organic material emplaced via precipitation from the atmosphere (e.g. Titan)  
706 or lodged in the surface as a result of cometary impacts into subsurface oceans. Titan's  
707 alkanological cycle and the associated meteorology creates a global distribution of trace species,  
708 evident in the formation and dynamics of clouds and an extensive photochemical haze in Titan's  
709 atmosphere, which affects the dynamics of how, when and where organic material settles on the  
710 surface and possibly interacts with the subsurface as seen in Figure 8.

711

712 **FIGURE 8**

713

714 In addition, cometary impacts could deliver key organics such as glycine, the simplest amino acid  
715 which has been detected on both comet 67P/Churyumov-Gerasimenko from *in situ* sampling by  
716 ESA's ROSETTA's mission and on comet 81P/Wild-2 from samples returned by NASA's Stardust  
717 mission. Neish et al. (2010) suggested that transient liquid water environments, created by impact  
718 melts could be an incubator for the deposited aerosols to create prebiotic chemistry. Further it is

719 likely that such impact melt pools could be stable for  $10^2$ – $10^4$  years (O'Brien et al. 2005).

720

721 This process could be circular; Tobie et al. (2012) suggests that some of the species now present  
722 in Titan's atmosphere may have originally been dissolved in the subsurface. On smaller ocean  
723 worlds such as Europa and Enceladus, the ocean may be in direct contact with the silicate core  
724 providing a means of water-rocks interactions (Mitri and Showman 2005; Iess et al. 2014). Recent  
725 detection of nanometer silica dust particles in Saturn's E-ring is indicative of an origin where  
726 alkaline high- temperature water-rock interactions is occurring (Hsu et al. 2015). The enormous  
727 heat output in the south polar terrain, associated with liquid water in contact with rocks, favors  
728 prebiotic processes, providing both an energy source and mineral surfaces for catalyzing chemical  
729 reactions.

730

731 Titan and Enceladus have already demonstrated remarkable astrobiological potential as evidenced  
732 by observations of Titan's complex atmosphere and methane cycle, analogous to Earth's water  
733 cycle, and Enceladus' cryovolcanic plume spewing rich organics from the subsurface out into  
734 space. Studies of the nature of these organics could tell us whether or not they are biogenic. For  
735 instance, part of the  $\text{CH}_4$  detected in the plume of Enceladus may result from methanogens  
736 analogous to those occurring in anaerobic chemosynthetic ecosystems on Earth (Stevens and  
737 McKinley 1995; McKay et al. 2008). A powerful method to distinguish between biogenic and  
738 abiogenic  $\text{CH}_4$  is to analyze the difference in carbon isotope,  $^{12}\text{C}/^{13}\text{C}$ , between  $\text{CH}_4$  and a potential  
739 source of C, most likely  $\text{CO}_2$  on Enceladus and Titan, and to analyze the pattern of carbon isotopes  
740 in other hydrocarbons, such as  $\text{C}_2\text{H}_6$ ,  $\text{C}_2\text{H}_4$ ,  $\text{C}_2\text{H}_2$ ,  $\text{C}_3\text{H}_8$  etc. (Sherwood et al. 2002; McKay et al.

741 2008). The abundances of other non-methane hydrocarbons relative to methane could also be used  
742 to distinguish between biological and other sources (McKay et al. 2008; McKay 2016). The  
743 detection of amino acids could provide additional evidence for active biogenic processes. Even  
744 though amino acids can be produced, both biologically and via aqueous alteration of refractory  
745 organics, their distribution pattern can confirm if they are of biological origin (Dorn et al. 2011).  
746 Indeed, low molecular weight amino acids, such as glycine and alanine, are kinetically favorable  
747 and therefore dominate mixture of amino acids synthesized by abiotic process, whereas amino  
748 acids resulting from biotic process show a more varied distribution dominated by the protein amino  
749 acids in roughly equal proportions (Dorn et al. 2011).

750

751 By searching for abnormal isotopic ratios and mass distribution of organic molecules, including  
752 amino acids, the proposed baseline mission can determine what chemical processes control the  
753 formation and evolution of complex organics on Titan and will test whether biotic processes are  
754 currently occurring inside Enceladus. The analysis of salts and minerals embedded in icy grains  
755 and their possible distribution throughout the plume will also provide crucial constraints on the  
756 nature of hydrothermal activity occurring in Enceladus' deep interior and on how it connects with  
757 the plume activity. The observations of Titan's surface will also reveal if active exchange processes  
758 with the interior is currently occurring and whether complex organics are potentially in contact  
759 with fresh water.

760

761 **4.6 Evidence for prebiotic and biotic chemical processes on Titan and Enceladus**

762 Unlike the other ocean worlds in the Solar System, Titan has a substantial atmosphere, consisting  
763 of approximately 95% nitrogen and 5% methane with trace quantities of hydrogen and its by-  
764 products such as hydrocarbons (e.g. ethane, acetylene, propane and diacetylene) and nitriles, (e.g.  
765 hydrogen cyanide (HCN) cyanoacetylene (HC<sub>3</sub>N) and cyanogen (C<sub>2</sub>N<sub>2</sub>)). Somewhat more complex  
766 molecules such as vinyl and ethylcyanide follow from these simpler units. In Titan's upper  
767 atmosphere, Cassini has detected large organic molecules with high molecular masses over 100 u.  
768 *In situ* measurements by the Cassini Plasma Spectrometer (CAPS) detected heavy positive ions  
769 (cations) up to 400 u (Crary et al. 2009) and heavy negative ions (anions) with masses up to 10,000  
770 u (Coates et al. 2007) in Titan's ionosphere. Whereas Cassini INMS only had the ability to detect  
771 cations, current high-resolution mass spectrometer technology can detect both cations and anions  
772 with much better mass resolution than Cassini-INMS, and even better mass resolution than  
773 Cassini-CAPS. It is thought that these heavy negative ions, along with other heavy molecules  
774 found in the upper atmosphere, are likely the precursors of aerosols that make up Titan's signature  
775 orange haze, possibly even precipitating to the surface. While the identities of these molecules are  
776 still unknown, their presence suggest a complex atmosphere that could hold the precursors for  
777 biological molecules such as those found on Earth. The ability to detect prebiotic molecules in  
778 Titan's atmosphere is currently limited by the mass range of the Cassini INMS to the two smallest  
779 biological amino acids, glycine (75 u) and alanine (89 u), and the limited mass resolution precludes  
780 any firm identification. However, Cassini INMS detected mass spectra fragments for positive ions  
781 at masses of 76 u and 90 u, which may be consistent with protonated glycine and alanine,  
782 respectively (Vuitton et al. 2007; Hörst et al. 2012). Experimental results from a Titan atmosphere  
783 simulation experiment found 18 molecules that could correspond to amino acids and nucleotide  
784 bases (Hörst et al. 2012). The proposed baseline mission would use high-resolution mass

785 spectrometry to measure heavy neutral and ionic constituents up to 1000 u, and the elemental  
786 chemistry of low-mass organic macromolecules and aerosols in Titan's upper atmosphere as well  
787 as monitor neutral-ionic chemical coupling processes.

788

789 The plume emanating from Enceladus' south pole probably contains the most accessible samples  
790 from an extra-terrestrial liquid water environment in the Solar System. The plume is mainly  
791 composed of water vapor and other gases: 0.91% H<sub>2</sub>O, 0.04% N<sub>2</sub>, 0.032% CO<sub>2</sub>, 0.016% CH<sub>4</sub>  
792 (Waite et al. 2006). In addition, complex macromolecular organic species with masses exceeding  
793 200 u, were detected in the plume emissions suggesting the presence of a thin organic-rich film on  
794 the upper layer of the ocean (Postberg et al., 2018). The presence of CO<sub>2</sub>, CH<sub>4</sub> and N<sub>2</sub> can constrain  
795 the oxidation state of Enceladus' hydrothermal system during its evolution. The minor gas  
796 constituents in the plume are indicative of high-temperature oxidation-reduction (redox) reactions  
797 in Enceladus' interior possibly a result of decay of short-lived radionuclides (Schubert et al.  
798 2007). In addition, H<sub>2</sub> production and escape may be a result of redox reactions. Further the high  
799 temperatures and H<sub>2</sub> escape may have led to the oxidation of NH<sub>3</sub> to N<sub>2</sub> (Glein et al. 2008).  
800 Enceladus' redox state may have or have had similarities with terrestrial submarine hydrothermal  
801 systems. Detection and inventory of reduced and oxidized species in the plume material (e.g.,  
802 NH<sub>3</sub>/N<sub>2</sub> ratio, H<sub>2</sub> abundance, reduced versus oxidized organic species) can constrain the redox  
803 state and evolution of Enceladus' hydrothermal system.

804

805 Cassini CDA measurements identified three types of grains in the plume and Saturn's E-ring. Type  
806 I and Type II grains are both salt-poor (Figure 9). Type I ice grains are nearly pure-water ice while  
807 Type II grains also possess silicates and organic compounds and Type III is salt-rich (0.5 – 2.0%  
808 by mass) (Postberg et al. 2009, 2011). The salinity of these particles suggests they originate in a  
809 place where likely water-rock interactions are taking place.

810

811 In addition, E-ring stream particles were identified as nanometer-sized SiO<sub>2</sub> (silica) dust particles  
812 that were initially embedded in plume ice grains (Hsu et al. 2015). These particles indicate an  
813 origin at locations where alkaline high temperature (>90°C) hydrothermal rock-water reactions are  
814 taking place (Hsu et al. 2015). Hsu et al. (2015) further suggests that a convective ocean is required  
815 to have silica nanoparticles transported from hydrothermal sites at the rocky core up to the surface  
816 of the ocean where they can be incorporated into icy plume grains. To confirm this hypothesis of  
817 current hydrothermal activity on Enceladus, a direct detection of silica and other minerals within  
818 ejected ice grains is required. SiO<sub>2</sub> nano-particles detected in Saturn's E-ring can now be much  
819 better investigated and quantified by high-resolution mass spectrometer with a higher dynamic  
820 range (10<sup>6</sup>–10<sup>8</sup>). In addition, with high resolution mass spectrometry in the proposed baseline  
821 mission it would also be possible to search for signatures of on-going hydrothermal activities from  
822 possible detection of native H<sub>2</sub> and He.

823

824 FIGURE 9

825

#### 826 4.7 Physical dynamics in Enceladus' plume and Titan's upper atmosphere

827 The total heat emission at the south polar “tiger stripes” is at least 5 GW (possibly up to 15 GW,  
828 Howett et al. 2011), and in some of the hot spots where jets emanate, the surface temperatures are  
829 as high as 200 K (Goguen et al. 2013). Cassini observations show that the plume is made up of  
830 ~100 discrete collimated jets as well as a diffuse distributed component (Hansen et al. 2008, 2011;  
831 Postberg et al. 2011; Porco et al. 2014). The majority of plume material can be found in the  
832 distributed diffuse portion of the plume, which likely originates from elongated fissures along  
833 Enceladus' tiger stripes while only a small portion of gas and grains are emitted from the jets  
834 (Hansen et al. 2011; Postberg et al. 2011). CDA measurements demonstrate that the majority of  
835 salt-poor grains tend to be ejected through the jets and at faster speeds while larger salt-rich grains  
836 tend to be ejected more slowly through the distributed portion of the plume (Postberg et al. 2011).  
837 Ice-to-vapor ratios can constrain how Enceladus' plume material is formed and transported to the  
838 surface. For example, ice-to-vapor ratios  $> 0.1$ – $0.2$  would exclude plume generation mechanisms  
839 which require a large amount of ice grains to be condensed from vapor (Ingersoll and Pankine  
840 2011; Porco et al. 2006). However, this ratio is poorly constrained with estimates ranging from  
841 0.05 (Schmidt et al. 2008) to 0.4 (Porco et al. 2006) to 0.35–0.7 (Ingersoll and Ewald 2011).  
842 Imaging and spectral mission from the proposed baseline mission could help constrain this  
843 important ratio. Cassini ISS images used to track plume brightness variation, which is proportional  
844 to the amount of grains in the plume, with the orbital position of Enceladus found more ice grains  
845 are emitted when Enceladus is near its farthest point from Saturn (apocenter). It is not understood  
846 if the plume vapor has such a variation. This temporal variation of the plume indicates that it is  
847 tidally driven but could also be due to possible physical libration (Hurford et al. 2009; Kite et al.  
848 2016). Kite et al. (2016) has suggested that the tiger stripe fissures are interspersed with vertical

849 pipe-like tubes with wide spacing that extend from the surface to the subsurface water. This  
850 mechanism allows tidal forces to turn water motion into heat, generating enough power to produce  
851 eruptions. in a sustained manner. High spatial resolution thermal emissions maps could be used to  
852 constrain the amount of energy dissipated between the tiger stripes

853

#### 854 **4.8 Geological evidence for interior-surface communication on Titan**

855 Geological features such as tectonic and putative cryovolcanic are the reflection of interior  
856 processes and may indicate communication between atmosphere-surface and subsurface enabling  
857 prebiotic/abiotic processes. Titan's surface offers a wealth of geological processes with which to  
858 constrain the extent that Titan's surface chemically communicates with its water-rich interior, in  
859 particular possible cryovolcanism and tectonics. Also of great importance to habitability are the  
860 transient H<sub>2</sub>O melt sheets and flows associated with impacts (e.g. Selk impact crater; Soderblom  
861 et al., 2010). On Titan, several features with volcanic landforms, lengthy flows, tall mountains,  
862 large caldera-like depressions, have been identified as possible cryovolcanic sites. At present, the  
863 Hotei Regio flows and the Sotra Patera region, which includes Sotra Patera, an elliptical deep  
864 depression on Titan, Mohini Fluctus, a lengthy flow feature, and Doom and Erebor Montes, two  
865 volcanic edifices, are considered to host the strongest candidates for cryovolcanism on Titan  
866 (Lopes et al. 2013). High resolution mapping (at minimum, 30 m/pixel with DTM vertical  
867 resolution of 10 m) of regions that are candidates for cryovolcanic activity could improve the  
868 ability to distinguish cryovolcanic features.

869



870 A variety of mountainous topography has been observed on Titan (Radebaugh et al. 2007; Cook-  
871 Hallett et al. 2015). The observed morphologies of many of Titan's mountain suggest contractional  
872 tectonism (Mitri et al. 2010; Liu et al. 2016). This is somewhat surprising, however, in that most  
873 tectonic landforms observed on other ocean worlds and icy satellites in the outer solar system  
874 appear to be extensional in nature. Understanding the tectonic regime of Titan is fundamental in  
875 understanding the transport of material between the moon's organic-rich surface and subsurface  
876 ocean and will also provide insight into the evolution of the other ocean worlds. We will test the  
877 hypothesis that Titan's mountains are formed by contraction by mapping the faults driving  
878 mountain formation in topographic context. A future mission can test the hypothesis that Titan's  
879 mountains are formed by contraction by mapping the faults driving mountain formation in  
880 topographic context by using the shape of the fault outcrop draped against topography to measure  
881 the faults' dip, which will be ~30 degrees to the horizontal for compressive mountains and ~60  
882 degrees for extensional mountains.

883

884 In addition to cryovolcanism and tectonism, which may transport water to Titan's surface, impact  
885 craters likely have created transient liquid-water environments on Titan's surface. Because of  
886 Titan's dense atmosphere, models suggest that melt sheets and flows associated with impact craters  
887 may remain liquid for  $10^4$ – $10^6$  years (Thompson and Sagan 1992; Artemieva and Lunine 2005),  
888 though the stability of such lakes is questioned (Senft and Stewart 2011; Zahnle et al. 2014) and  
889 detailed imaging of the floors of young craters is needed to constrain these models.

890

## 891 5. Science case for the option 1 and 2 mission scenarios

### 892 5.1 *In situ* Titan sea probe/lander

893 Titan presents approximately 600 standing bodies of liquid hydrocarbons at the polar regions  
894 forming seas and lakes (Stofan et al. 2007; Lopes et al. 2018) which are found poleward of 55°  
895 latitude and cover 1.2% of the surface that has been observed (~50%) by Cassini's instruments  
896 (Hayes et al. 2008, 2011). Seasonal asymmetry likely due to Saturn's current orbital configuration  
897 (Aharonson et al. 2009) has resulted in the majority of lakes, filled and empty, being located in the  
898 north pole while empty and paleo-lakes predominate in the south pole. In the north, 87% of the  
899 area of observed liquid deposits are contained within the three largest lakes, Ligeia, Kraken, and  
900 Punga Mare, which are similar in size to the Great Lakes (USA). This hemispheric asymmetry of  
901 lakes and seas yields a net transport of volatiles (methane/ethane) from the south to the north;  
902 however, as the orbital parameters shift the net flux of northward-bound volatiles is expected to  
903 slow and eventually reverse, resulting in a larger southern hemispheric liquid distribution in ~35  
904 kyr. If this hypothesis is correct, the distribution of liquid deposits on Titan is expected to move  
905 between the poles with a period of ~50 kyr in a process analogous to Croll-Milankovich cycles on  
906 Earth. *In situ* measurement and comparison between the relative abundance of volatiles that are  
907 mobile over these timescales (e.g., methane, ethane) versus those that are involatile (e.g., propane,  
908 benzene), can be used to test this hypothesis and understand volatile transport on thousand years  
909 timescale. Volatile transport over shorter timescales (diurnal, tidal, and seasonal) can be  
910 investigated via *in situ* measurements of the methane evaporation rate and associated  
911 meteorological conditions (e.g., wind speed, temperature, humidity). These measurements can be  
912 used to ground-truth methane transport predictions from global climate models (e.g., Mitchell et

913 al. 2008; Tokano et al. 2009; Schneider et al. 2012). Cassini RADAR altimetry results have been  
914 used to determine the depth and constrain the composition of the Ligeia Mare (Mastrogiuseppe et  
915 al. 2014) and Winnepeg Lacus (Mastrogiuseppe et al. 2019) at the north pole and Ontario Lacus  
916 at the south pole (Mastrogiuseppe et al. 2018). *In situ* sounding of one of the northern seas can be  
917 used to confirm the depth and composition of Ligeia Mare or else to determine the depth of the  
918 Kraken Mare, Titan's largest sea, thus improving our understanding of the total volume of liquid  
919 available for interaction with the atmosphere. The inventory of methane in Titan's Mare, which  
920 requires knowledge of both depth and composition, will provide a lower limit on the length of time  
921 that the lakes can sustain methane in Titan's atmosphere (Mitri et al. 2007) and help to quantify  
922 the required rate of methane resupply from the interior and/or crust. Similarly, the absolute  
923 abundance of methane photolysis products (e.g., ethane, propane) will determine a lower limit for  
924 the length of time that methane has been abundant enough to drive photolysis in the upper  
925 atmosphere and deposit its products onto the surface and, ultimately, into the lakes and seas.

926

927 Similar to the Earth's oceans, Titan's seas record a history of their parent body's origin and  
928 evolution. Specifically, the noble gas and isotopic composition of the sea can provide information  
929 regarding the origin of Titan's atmosphere, reveal the extent of communication with the interior,  
930 potentially constrain the conditions in the Saturn system during formation, and refine estimates of  
931 the methane outgassing history. Titan's lakes and seas collect organic material both directly,  
932 through atmospheric precipitation of photolysis products, and indirectly, through aeolian or fluvial  
933 transport of surface materials (e.g., river systems flowing into the Mare). As a result, the lakes and  
934 seas represent the most complete record of Titan's organic complexity and present a natural

935 laboratory for studying prebiotic organic chemistry (Lunine et al. 2010). Titan's environment is  
936 similar to conditions on Earth four billion year ago and presents an opportunity to study active  
937 systems involving several key compounds of prebiotic chemistry (Schulze–Makuch and  
938 Grinspoon 2005; Raulin 2008; Coustenis and Raulin, 2015). Noble gas measurements and, isotopic  
939 ratios can also be used to decipher the history of Titan's atmosphere. For example, the  $^{13}\text{C}/^{12}\text{C}$   
940 ratio of methane was used by Niemann et al. (2010) to conclude that methane last outgassed from  
941 the interior  $\sim 10^7$  years ago. However, this calculation assumes that the exposed methane reservoir  
942 has an isotopic composition that is in equilibrium with the atmosphere. If the carbon isotope ratio  
943 of hydrocarbons in Titan's lakes/seas were found to be different than in the atmosphere, it would  
944 imply chemical alteration of the isotopic composition and indicate a different timescale for the  
945 history of methane-outgassing.

946

947 In summary, *in situ* exploration of Titan's lakes and seas will address fundamental questions  
948 involving the origin, evolution, and history of both Titan and the broader Saturnian system. The  
949 study of Titan's organic chemistry has direct applicability to our understanding of early prebiotic  
950 chemistry on Earth, allowing the investigation of reactions and timescales inaccessible to terrestrial  
951 labs.

952

## 953 **5.2 Ice penetrating radar (IPR)**

954 The ice penetrating radar (IPR) would be capable of both shallow and deep sounding to  
955 characterize the subsurface with a depth of 9 km and  $\sim 30$  m vertical resolution at minimum. An

956 IPR can characterize structural, compositional and thermal variations occurring in the subsurface  
957 providing data that can correlate surface and subsurface features and processes, deformation in the  
958 upper ice shell, as well as global and local surface age. On Titan, radar sounder observations with  
959 a penetration depth up to ~9 km with a vertical resolution of ~30 m, similar to JUICE RIME and  
960 Europa Clipper REASON, could directly determine the relict Brittle-Ductile transition of the ice  
961 shell revealing its thermal state, thus constraining its ice shell thickness and thermal evolution. Liu  
962 et al. (2016) suggests that subsurface liquid hydrocarbons could enable contractional structures to  
963 form on Titan without the necessity of large stresses. An IPR would be able to detect any near  
964 surface pockets of liquid. In addition, an IPR would also investigate the ice-ocean interface at  
965 Enceladus' SPT and its variability in the SPT.

966

967 An additional option for radar architecture could be a multi-mode radar design suitable for both  
968 sounding and imaging to be operated in two modes: a vertical sounder mode, with similar  
969 capabilities as described above but with different architecture, and a Synthetic Aperture Radar  
970 (SAR) imaging mode, similar to Cassini's, but with higher resolution at tens of meters. The  
971 additional SAR mode could be used for high-resolution imaging of the surface, complementing  
972 the IR imaging, as well as for creating three dimensional high resolution bathymetric maps of Titan  
973 seas and lakes and could permit investigation of any possible compositional variation in space and  
974 time of the hydrocarbon liquid and/or sea floor properties.

975

976

977 **References**

- 978 Aharonson, O., et al. 2009. An asymmetric distribution of lakes on Titan as a possible consequence  
979 of orbital forcing. *Nature Geoscience* 2, 851-854.
- 980 Artemieva, N., Lunine, J.I. 2005. Impact cratering on Titan II. Global melt, escaping ejecta, and  
981 aqueous alteration of surface organics. *Icarus* 175, 522-533.
- 982 Atreya, S.K., et al. 2006. Titan's methane cycle. *Planetary and Space Science* 54, 1177-1187.
- 983 Barco, A., et al. 2019. Design and Development of the ESA Am-Fueled Radioisotope Power  
984 Systems. *IEEE Aerospace Conference*, 1-11.
- 985 Barnes, J.W., et al. 2014. Cassini/VIMS observes rough surfaces on Titan's Punga Mare in  
986 specular reflection. *Planetary Science*, 3(1), p.1.
- 987 Barnes, J. W. et al. 2011. Organic sedimentary deposits in Titan's dry lakebeds: Probable  
988 evaporite. *Icarus*, 216(1), 136-140.
- 989 Barnes, J.W., et al. 2013. A transmission spectrum of Titan's north polar atmosphere from a  
990 specular reflection of the Sun. *The Astrophysical Journal*, 777:161.
- 991 Beghin, C., et al. 2012. Analytic theory of Titan's Schumann resonance: Constraints on ionospheric  
992 conductivity and buried water ocean. *Icarus* 218, 1028-1042.
- 993 Bèzard, B. 2014. The methane mole fraction in Titan's stratosphere from DISR measurements  
994 during the Huygens probe's descent. *Icarus* 242, 64-73.

995 Birch, S., et al. 2016. Geomorphologic Mapping of Titan's Polar Terrains: Constraining Surface  
996 Processes and Landscape Evolution. *Icarus*.

997 Birch, S. P. D. et al. 2018 Raised Rims around Titan's Sharp-Edged Depressions. *Geophysical*  
998 *Research Letters* 45.

999 Blankenship, D. D., et al. 2009. Radar sounding of Europa's subsurface properties and processes:  
1000 The view from Earth. In *Europa* (pp. 631-654). Univ. Arizona Press.

1001 Brown, R. H. et al. 2008. The identification of liquid ethane in Titan's Ontario Lacus. *Nature*,  
1002 454(7204), 607.

1003 Bruzzone, L., et al. 2013. RIME: Radar for icy moon exploration. In 2013 IEEE International  
1004 Geoscience and Remote Sensing Symposium- IGARSS (pp. 3907-3910). IEEE.

1005 Bruzzone, L., et al. 2015. Jupiter icy moon explorer (JUICE): Advances in the design of the radar  
1006 for icy moons (rime). In 2015 IEEE International Geoscience and Remote Sensing Symposium-  
1007 IGARSS (pp. 1257-1260).

1008 Brzobohaty, T. et al. 2016. Effect of ice-shell thickness variations on the tidal response of Saturn's  
1009 moon Enceladus, *Icarus*.

1010 Burr, D.M. et al. 2006. Sediment transport by liquid surficial flow: Application to Titan. *Icarus*  
1011 181, 235-242.

1012 Burr, D.M., et al. 2013. Morphology of fluvial networks on Titan: Evidence for structural control.  
1013 *Icarus* 226, 742-759.

- 1014 Cable, M.L., et al. 2014. Experimental determination of the kinetics of formation of the benzene-  
1015 ethane co-crystal and implications for Titan. *Geophysical Research Letters* 41, 5396-5401.
- 1016 Cable, M.L., et al. 2020. Properties and Behavior of the Acentonitrile-Acetylene Co-Crystal Under  
1017 Titan Surface Conditions. *ACS Earth and Space Chemistry*
- 1018 Čadek, O., and 10 colleagues 2016. Enceladus's internal ocean and ice shell constrained from  
1019 Cassini gravity, shape, and libration data. *Geophysical Research Letters* 43, 5653-5660.
- 1020 Čadek, O., et al. 2019. Long-term stability of Enceladus' uneven ice shell. *Icarus*, 319, 476-484.
- 1021 Clark, R.N., et al. 2010. Detection and mapping of hydrocarbon deposits on Titan. *Journal of*  
1022 *Geophysical Research: Planets*, 115(E10).
- 1023 Coates, A.J., et al. 2007. Discovery of heavy negative ions in Titan's ionosphere. *Geophysical*  
1024 *Research Letters* 34, L22103.
- 1025 Cook-Hallett, C., et al. 2015. Global contraction/expansion and polar lithospheric thinning on  
1026 Titan from patterns of tectonism. *Journal of Geophysical Research (Planets)* 120, 1220-1236.
- 1027 Cordier, D., et al. 2010. About the Possible Role of Hydrocarbon Lakes in the Origin of Titan's  
1028 Noble Gas Atmospheric Depletion. *The Astrophysical Journal* 721, L117-L120.
- 1029 Cornet, T., et al. 2015. Dissolution on Titan and on Earth: Toward the age of Titan's karstic  
1030 landscapes. *Journal of Geophysical Research (Planets)* 120, 1044-1074.
- 1031 Coustenis, et al. 2009. TandEM: Titan and Enceladus mission. *Exp. Astron.* 23, 893–946.



- 1032 Coustenis, A., et al. "The Joint NASA-ESA Titan Saturn System Mission (TSSM)  
1033 Study." *LPI* (2009): 1060.
- 1034 Coustenis, A., Raulin, F. 2015. "Titan Astrobiology". *In the Encyclopedia of Astrobiology*, 2nd  
1035 edition, M. Gargaud, R. Amils, J. Cernicharo, H. J. Cleaves II, K. Kobayashi, D. Pinti, M. Viso  
1036 (Eds), Springer, 2550 p., ISBN 978-3-662-44184-8.
- 1037 Coustenis, A. 2015. "The Cassini-Huygens mission". *In the Encyclopedia of Astrobiology*, 2nd  
1038 edition, M. Gargaud, R. Amils, J. Cernicharo, H. J. Cleaves II, K. Kobayashi, D. Pinti, M. Viso  
1039 (Eds), Springer, 2550 p., ISBN 978-3-662-44184-8.
- 1040 Crary, F.J., et al. 2009. Heavy ions, temperatures and winds in Titan's ionosphere: Combined  
1041 Cassini CAPS and INMS observations. *Planetary and Space Science* 57, 1847-1856.
- 1042 Davies, A.G., et al. 2016. Cryolava flow destabilization of crustal methane clathrate hydrate on  
1043 Titan. *Icarus* 274, 23-32.
- 1044 De Sanctis et al. 2020. Relict Ocean Worlds: Ceres. *Space Science Reviews* 216, 60
- 1045 Dorn, E.D., Adami, C. 2011. Robust Monomer- Distribution Biosignatures in Evolving Digital  
1046 Biota. *Astrobiology* 11, 959-968.
- 1047 Dougherty, M.K., et al. 2006. Identification of a Dynamic Atmosphere at Enceladus with the  
1048 Cassini Magnetometer. *Science* 311, 1406-1409.
- 1049 Dougherty, M.K., et al. 2010 Titan Beyond Cassini-Huygens. *Titan from Cassini-Huygens*, 479-  
1050 488.
- 1051 Elachi, C., et al. 2004. Radar: The Cassini Titan Radar Mapper. *Space Sci. Rev.* 115, 71–110.

1052 Gebara, C. A., et al. 2019. Tensegrity Ocean World Landers. In AIAA Scitech 2019 Forum (p.  
1053 0868).

1054 Gladstone, G. R., et al. 2016. The atmosphere of Pluto as observed by New Horizons. *Science*,  
1055 351(6279), aad8866.

1056 Glein, C.R., et al. 2008. The oxidation state of hydrothermal systems on early Enceladus. *Icarus*  
1057 197, 157-163.

1058 Glein, C.R., et al. 2015. The pH of Enceladus' ocean. *Geochimica et Cosmochimica Acta* 162,  
1059 202-219.

1060 Goguen, J.D., and 12 colleagues 2013. The temperature and width of an active fissure on Enceladus  
1061 measured with Cassini VIMS during the 14 April 2012 South Pole flyover. *Icarus* 226, 1128-1137.

1062 Griffith, C.A., Zahnle, K. 1995. Influx of cometary volatiles to planetary moons: The atmospheres  
1063 of 1000 possible Titans. *Journal of Geophysical Research* 100, 16907-16922.

1064 Grima, C., et al. 2015. Radar signal propagation through the ionosphere of Europa. *Planetary and*  
1065 *Space Science*, 117, 421-428.

1066 Gudipati, M. S., et al. 2013. Photochemical activity of Titan's low-altitude condensed haze. *Nature*  
1067 *Communications*. 4:1648, DOI: 10.1038/ncomms2649.

1068 Griffith, C. A., et al. 2019. A corridor of exposed ice-rich bedrock across Titan's tropical region.  
1069 *Nature Astronomy*, 1.

- 1070 Hand, K.P., Sotin, C., Hayes, A., Coustenis, A. 2020 On the Habitability and Future Exploration  
1071 of Ocean Worlds. *Space Science Reviews* 216, Issue 4, in press.
- 1072 Hansen, C.J., et al. 2006. Enceladus' Water Vapor Plume. *Science* 311, 1422-1425.
- 1073 Hansen, C.J., et al. 2008. Water vapour jets inside the plume of gas leaving Enceladus. *Nature* 456,  
1074 477-479.
- 1075 Hansen, C.J., and 10 colleagues 2011. The composition and structure of the Enceladus plume.  
1076 *Geophysical Research Letters* 38, L11202.
- 1077 Hayes, A., et al. 2008. Hydrocarbon lakes on Titan: Distribution and interaction with a porous  
1078 regolith. *Geophysical Research Letters* 35, L09204.
- 1079 Hayes, A.G., and 11 colleagues 2010. Bathymetry and absorptivity of Titan's Ontario Lacus.  
1080 *Journal of Geophysical Research (Planets)* 115, E09009.
- 1081 Hayes, A.G., and 14 colleagues 2011. Transient surface liquid in Titan's polar regions from  
1082 Cassini. *Icarus* 211, 655-671.
- 1083 Hayes, A. G., et al. 2017. Topographic constraints on the evolution and connectivity of Titan's  
1084 lacustrine basins. *Geophysical Research Letters*, 44(23), 11-745.
- 1085 Hedman, M.M., et al. 2009. Spectral Observations of the Enceladus Plume with Cassini-Vims.  
1086 *The Astrophysical Journal* 693, 1749-1762.

- 1087 Heggy, E., et al. 2006. Ground-penetrating radar sounding in mafic lava flows: Assessing  
1088 attenuation and scattering losses in Mars-analog volcanic terrains. *Journal of Geophysical*  
1089 *Research: Planets*, 111(E6).
- 1090 Hörst, S.M., et al. 2008. Origin of oxygen species in Titan's atmosphere. *Journal of Geophysical*  
1091 *Research (Planets)* 113, E10006.
- 1092 Hörst, S.M., and 12 colleagues 2012. Formation of Amino Acids and Nucleotide Bases in a Titan  
1093 Atmosphere Simulation Experiment. *Astrobiology* 12, 809-817.
- 1094 Howett, C.J.A., et al. 2011. High heat flow from Enceladus' south polar region measured using 10  
1095  $-600\text{ cm}^{-1}$  Cassini/CIRS data. *Journal of Geophysical Research (Planets)* 116, E03003.
- 1096 Hsu, H.-W. et al. 2011. Stream particles as the probe of the dust-plasma-magnetosphere interaction  
1097 at Saturn. *Journal of Geophysical Research (Space Physics)* 116, A09215.
- 1098 Hsu, H.-W., et al. 2014. Silica Nanoparticles Provide Evidence for Hydrothermal Activities at  
1099 Enceladus. *Workshop on the Habitability of Icy Worlds 1774*, 4042.
- 1100 Hsu, H.-W., and 14 colleagues 2015. Ongoing hydrothermal activities within Enceladus. *Nature*  
1101 519, 207-210.
- 1102 Hurford, T.A., et al. 2009. Geological implications of a physical libration on Enceladus. *Icarus*  
1103 203, 541-552.
- 1104 Iess, L., et al. 2010. Gravity Field, Shape, and Moment of Inertia of Titan. *Science* 327, 1367.
- 1105 Iess, L., et al. 2012. The Tides of Titan. *Science* 337, 457.

1106 Iess, L., and 10 colleagues 2014. The Gravity Field and Interior Structure of Enceladus. *Science*  
1107 344, 78-80.

1108 Ingersoll, A.P., Pankine, A.A. 2010. Subsurface heat transfer on Enceladus: Conditions under  
1109 which melting occurs. *Icarus* 206, 594-607.

1110 Ingersoll, A.P., Ewald, S.P. 2011. Total particulate mass in Enceladus plumes and mass of Saturn's  
1111 E ring inferred from Cassini ISS images. *Icarus* 216, 492-506.

1112 Israël, G., et al. 2005. Complex organic matter in Titan's atmospheric aerosols from in situ  
1113 pyrolysis and analysis. *Nature*, 438(7069), 796.

1114 Jennings, D.E., et al. 2009.  $^{12}\text{C}/^{13}\text{C}$  Ratio in Ethane on Titan and Implications for Methane's  
1115 Replenishment. *Journal of Physical Chemistry A* 113, 11101-11106.

1116 Kite, E.S., Rubin, A.M. 2016. Sustained eruptions on Enceladus explained by turbulent dissipation  
1117 in tiger stripes. *Proceedings of the National Academy of Science* 113, 3972-3975.

1118 Le Gall, A., et al. 2017. Thermally anomalous features in the subsurface of Enceladus's south polar  
1119 terrain. *Nature Astronomy*, 1(4), 0063.

1120 Liu, Z.Y.C., et al. 2016. The tectonics of Titan: Global structural mapping from Cassini RADAR.  
1121 *Icarus* 270, 14-29.

1122 Lopes, R.M.C., and 43 colleagues 2007. Cryovolcanic features on Titan's surface as revealed by  
1123 the Cassini Titan Radar Mapper. *Icarus* 186, 395-412.

1124 Lopes, R.M.C., and 15 colleagues 2013. Cryovolcanism on Titan: New results from Cassini  
1125 RADAR and VIMS. *Journal of Geophysical Research (Planets)* 118, 416-435.

1126 Lopes, R. M. C., et al. 2019. Titan as Revealed by the Cassini Radar. *Space Science Reviews*,  
1127 215(4), 33.

1128 Lorenz, R.D., and 39 colleagues 2006. The Sand Seas of Titan: Cassini RADAR Observations of  
1129 Longitudinal Dunes. *Science* 312, 724-727.

1130 Lorenz, Ralph D., and Newman, Claire E. 2015. Twilight on Ligeia: Implications of  
1131 communications geometry and seasonal winds for exploring Titan’s seas 2020–2040” *Advances*  
1132 *in Space Research*, 56, Issue 1, 190-204.

1133 Lorenz, Ralph D., and J. Mann. 2015. Seakeeping on Ligeia Mare: dynamic response of a floating  
1134 capsule to waves on the hydrocarbon seas of Saturn's moon Titan. *Johns Hopkins/APL Technical*  
1135 *Digest* 33.2, 82-94.

1136 Lorenz, R. D., et al. 2015. Instrumented splashdown testing of a scale model titan Mare Explorer  
1137 (tiME) capsule. *The Aeronautical Journal* 119.1214, 409-431.

1138 Lorenz, R. D., and N. A. Cabrol. 2018. Onboard science insights and vehicle dynamics from scale-  
1139 model trials of the Titan Mare Explorer (TIME) capsule at Laguna Negra, Chile. *Astrobiology*  
1140 18.5, 607-618.

1141 Lorenz, Ralph D., et al. 2018. Dragonfly: a Rotorcraft Lander Concept for scientific exploration  
1142 at Titan. *Johns Hopkins APL Technical Digest*.

- 1143 Lunine, J., et al. 1983. Ethane Ocean on Titan. *Science* 222, 1229–1230.
- 1144 Lunine, J.I., Stevenson, D.J. 1987. Clathrate and ammonia hydrates at high pressure - Application  
1145 to the origin of methane on Titan. *Icarus* 70, 61- 77.
- 1146 Lunine, J., et al. 2010. The Origin and Evolution of Titan. *Titan from Cassini-Huygens* 35.
- 1147 Lunine, J. I. 2017. Ocean worlds exploration. *Acta Astronautica*, 131, 123-130.
- 1148 Lunine, J., et al. 2018. “Future exploration of Enceladus and other Saturnian moons”. *In*  
1149 “Enceladus and the Icy Moons of Saturn”. LPI/UA/Space Science Series, Paul M. Schenk, Roger  
1150 N. Clark, Carly J. A. Howett, Anne J. Verbiscer, J. Hunter Waite Eds., ISBN 9780816537075.
- 1151 MacKenzie, S.M., and 10 colleagues 2014. Evidence of Titan's climate history from evaporite  
1152 distribution. *Icarus* 243, 191-207.
- 1153 Malaska, M.J., et al. 2016. Material transport map of Titan: The fate of dunes. *Icarus* 270, 183-  
1154 196.
- 1155 Malaska, M. J. 2017. Topographic constraints on the evolution and connectivity of Titan's  
1156 lacustrine basins. *Geophysical Research Letters*, 44(23), 11- 745.
- 1157 Mandt, K.E., and 18 colleagues 2012. Ion densities and composition of Titan's upper atmosphere  
1158 derived from the Cassini Ion Neutral Mass Spectrometer: Analysis methods and comparison of  
1159 measured ion densities to photochemical model simulations. *Journal of Geophysical Research*  
1160 (Planets) 117, E10006.

1161 Mastrogiuseppe, M. et al. 2014. The bathymetry of a Titan sea. *Geophys. Res. Lett.* 41, 1432–  
1162 1437.

1163 Mastrogiuseppe, M., et al. 2019. Deep and methane-rich lakes on Titan. *Nature Astronomy*, 3(6),  
1164 535.

1165 Mastrogiuseppe, M., Hayes, A. G., Poggiali, V., Lunine, J. I., Lorenz, R. D., Seu, R., ... & Birch,  
1166 S. P. 2018. Bathymetry and composition of Titan's Ontario Lacus derived from Monte Carlo-based  
1167 waveform inversion of Cassini RADAR altimetry data. *Icarus*, 300, 203-209.

1168 McKay, C.P., et al. 2008. The Possible Origin and Persistence of Life on Enceladus and Detection  
1169 of Biomarkers in the Plume. *Astrobiology* 8, 909- 919.

1170 McKay, C.P. 2016. Titan as the Abode of Life. *Life*, 6, 8.

1171 McKinnon, W.B. 2015. Effect of Enceladus's rapid synchronous spin on interpretation of Cassini  
1172 gravity. *Geophysical Research Letters* 42, 2137-2143.

1173 Miller, K. et al. 2019. Contributions from accreted organics to Titan's atmosphere: New insights  
1174 from cometary and chondritic data. *The Astrophysical Journal*. doi:10.3847/1538-4357/aaf561.

1175 Mitchell, J. L., et al. 2011. Locally enhanced precipitation organized by planetary-scale waves on  
1176 Titan. *Nature Geoscience*, 4(9), 589.

1177 Mitri, G., Showman, A.P . 2005. Convective conductive transitions and sensitivity of a convecting  
1178 ice shell to perturbations in heat flux and tidal-heating rate: Implications for Europa. *Icarus* 177,  
1179 447-460.



1180 Mitri, G., et al. 2007. Hydrocarbon lakes on Titan. *Icarus* 186, 385-394.

1181 Mitri, G., Showman, A. P. 2008. Thermal convection in ice-I shells of Titan and Enceladus. *Icarus*,  
1182 193(2), 387-396.

1183 Mitri, G., et al. 2010. Mountains on Titan: Modeling and observations. *Journal of Geophysical*  
1184 *Research (Planets)* 115, E10002.

1185 Mitri, G., and 16 colleagues 2014a. The exploration of Titan with an orbiter and a lake probe.  
1186 *Planetary and Space Science* 104, 78-92.

1187 Mitri, G., et al. 2014b. Shape, topography, gravity anomalies and tidal deformation of Titan. *Icarus*  
1188 236, 169-177.

1189 Mitri, G., et al. 2018. Explorer of Enceladus and Titan (E2T): Investigating ocean worlds' evolution  
1190 and habitability in the solar system. *Planetary and space science*, 155, 73-90.

1191 Mitri, G., et al. 2019. Possible explosive crater origin of small lake basins with raised rims on  
1192 Titan. *Nature Geoscience* 12, 791-796.

1193 Moore, J.M., Howard, A.D. 2010. Are the basins of Titan's Hotei Regio and Tui Regio sites of  
1194 former low latitude seas?. *Geophysical Research Letters* 37, L22205.

1195 Mousis, O., et al. 2002. An Evolutionary Turbulent Model of Saturn's Subnebula: Implications for  
1196 the Origin of the Atmosphere of Titan. *Icarus* 156, 162-175.

1197 Mousis, O., Schmitt, B. 2008. Sequestration of Ethane in the Cryovolcanic Subsurface of Titan.  
1198 *The Astrophysical Journal* 677, L67.

1199 Mousis, O., and 10 colleagues 2009. Clathration of Volatiles in the Solar Nebula and Implications  
1200 for the Origin of Titan's Atmosphere. *The Astrophysical Journal* 691, 1780-1786.

1201 Mousis, O., et al. 2011. Removal of Titan's Atmospheric Noble Gases by Their Sequestration in  
1202 Surface Clathrates. *The Astrophysical Journal* 740, L9.

1203 Neish, C.D., et al. 2010. Titan's Primordial Soup: Formation of Amino Acids via Low-Temperature  
1204 Hydrolysis of Tholins. *Astrobiology* 10, 337-347.

1205 Neish, C.D., Lorenz, R.D. 2012. Titan's global crater population: A new assessment. *Planetary  
1206 and Space Science* 60, 26-33.

1207 Neish, C.D., and 14 colleagues 2015. Spectral properties of Titan's impact craters imply chemical  
1208 weathering of its surface. *Geophysical Research Letters* 42, 3746-3754.

1209 Neish, C.D., et al. 2016. Fluvial erosion as a mechanism for crater modification on Titan. *Icarus*  
1210 270, 114-129.

1211 Niemann, H.B., and 17 colleagues 2005. The abundances of constituents of Titan's atmosphere  
1212 from the GCMS instrument on the Huygens probe. *Nature* 438, 779-784.

1213 Niemann, H.B., et al. 2010. Composition of Titan's lower atmosphere and simple surface volatiles  
1214 as measured by the Cassini-Huygens probe gas chromatograph mass spectrometer experiment.  
1215 *Journal of Geophysical Research (Planets)* 115, E12006.

1216 Nimmo, F., Pappalardo, R.T. 2016. Ocean worlds in the outer solar system, *J. Geophys. Res.*

- 1217 Nixon, C.A., and 12 colleagues 2012. Isotopic Ratios in Titan's Methane: Measurements and  
1218 Modeling. *The Astrophysical Journal* 749, 159.
- 1219 Nixon, C. A. et al. 2018. Titan's cold case files- Outstanding questions after Cassini-Huygens.  
1220 *Planetary and Space Science*, 155, 50.
- 1221 O'Brien, D.P., et al. 2005. Numerical calculations of the longevity of impact oases on Titan. *Icarus*  
1222 173, 243-253.
- 1223 Ono, T., et al. 2010. The Lunar Radar Sounder (LRS) Onboard the KAGUY A (SELENE)  
1224 Spacecraft. *Space Science Reviews* 154.1-4, 145- 192.
- 1225 Oriti, Sal, and Paul Schmitz. 2019. Dynamic RPS Path to Flight.
- 1226 Owen, T., Niemann, H.B. 2009. The origin of Titan's atmosphere: some recent advances.  
1227 *Philosophical Transactions of the Royal Society of London Series A* 367, 607-615.
- 1228 Picardi, G., et al. 2004. Performance and surface scattering models for the Mars Advanced Radar  
1229 for Subsurface and Ionosphere Sounding (MARSIS). *Planetary and Space Science* 52.1-3, 149-  
1230 156.
- 1231 Poggiali, V., Mastrogiuseppe, M., Hayes, A. G., Seu, R., Birch, S. P. D., Lorenz, R., ... &  
1232 Hofgartner, J. D. (2016). Liquid-filled canyons on Titan. *Geophysical Research Letters*, 43(15),  
1233 7887-7894.
- 1234 Porco, C.C., and 24 colleagues 2006. Cassini Observes the Active South Pole of Enceladus.  
1235 *Science* 311, 1393-1401.

- 1236 Porco, C., et al. 2014. How the Geysers, Tidal Stresses, and Thermal Emission across the South  
1237 Polar Terrain of Enceladus are Related. *The Astronomical Journal* 148, 45.
- 1238 Postberg, F., et al. 2008. The E-ring in the vicinity of Enceladus. II. Probing the moon's interior.  
1239 The composition of E-ring particles. *Icarus* 193, 438- 454.
- 1240 Postberg, F., et al. 2009. Sodium salts in E-ring ice grains from an ocean below the surface of  
1241 Enceladus. *Nature* 459, 1098-1101.
- 1242 Postberg, F., et al. 2011. A salt-water reservoir as the source of a compositionally stratified plume  
1243 on Enceladus. *Nature* 474, 620-622.
- 1244 Postberg, F., et al. 2015. Refractory Organic Compounds in Enceladus' Ice Grains and  
1245 Hydrothermal Activity. AGU Fall Meeting Abstracts.
- 1246 Postberg, F., et al. 2018. Macromolecular organic compounds from the depths of Enceladus.  
1247 *Nature* 558, 564-568.
- 1248 Radebaugh, J., et al. 2007. Mountains on Titan observed by Cassini Radar. *Icarus* 192, 77-91.
- 1249 Radebaugh, J., and 15 colleagues 2008. Dunes on Titan observed by Cassini Radar. *Icarus* 194,  
1250 690- 703.
- 1251 Raulin, F. 2008. Organic lakes on Titan. *Nature* 454, 587-589.
- 1252 Roth, L., Saur, et al. 2014. Transient Water Vapor at Europa's South Pole. *Science* 343, 171-174.

1253 Roth, L., et al. 2017. Detection of a hydrogen corona in HST Ly $\alpha$  images of Europa in transit of  
1254 Jupiter. *The Astronomical Journal*, 153(2), 67.

1255 Schmidt, J., et al. 2008. Slow dust in Enceladus' plume from condensation and wall collisions in  
1256 tiger stripe fractures. *Nature* 451, 685-688.

1257 Schneider, T., et al. 2012. Polar methane accumulation and rainstorms on Titan from simulations  
1258 of the methane cycle. *Nature*, 481(7379), 58.

1259 Schubert, G., et al. 2007. Enceladus: Present internal structure and differentiation by early and  
1260 long-term radiogenic heating. *Icarus* 188, 345- 355.

1261 Schulze-Makuch, D., Grinspoon, D. H. (2005). Biologically enhanced energy and carbon cycling  
1262 on Titan?. *Astrobiology*, 5(4), 560-567.

1263 Senft, L.E., Stewart, S.T. 2011. Modeling the morphological diversity of impact craters on icy  
1264 satellites. *Icarus* 214, 67-81.

1265 Seu, R., et al. 2007. SHARAD sounding radar on the Mars Reconnaissance Orbiter. *Journal of*  
1266 *Geophysical Research: Planets*, 112(E5).

1267 Sherwood L., et al. 2002. Abiogenic formation of alkanes in the Earth's crust as a minor source for  
1268 global hydrocarbon reservoirs. *Nature* 416, 522- 524.

1269 Soderblom, L.A., and 26 colleagues 2007. Correlations between Cassini VIMS spectra and  
1270 RADAR SAR images: Implications for Titan's surface composition and the character of the  
1271 Huygens Probe Landing Site. *Planetary and Space Science* 55, 2025-2036.

1272 Soderblom, J.M., et al. 2010. Geology of the Selk crater region on Titan from Cassini VIMS  
1273 observations. *Icarus*, 208, 905–912.

1274 Soderblom, L.A., et al. 1990. Triton's geyser-like plumes - Discovery and basic characterization.  
1275 *Science* 250, 410-415.

1276 Soderblom, J.M., et al. 2012. Modeling specular reflections from hydrocarbon lakes on Titan.  
1277 *Icarus*, 220(2), pp.744-751.

1278 Solomonidou, A., et al. 2019. Spectral and emissivity analysis of the raised ramparts around Titan's  
1279 northern lakes. *Icarus*, in press.

1280 Sotin, C., et al. "JET: Journey to Enceladus and Titan." *LPI* 1608 (2011): 1326.

1281 Spahn, F., and 15 colleagues 2006. Cassini Dust Measurements at Enceladus and Implications for  
1282 the Origin of the E Ring. *Science* 311, 1416-1418.

1283 Spilker, L. (2019). Cassini-Huygens' exploration of the Saturn system: 13 years of discovery.  
1284 *Science*, 364(6445), 1046-1051.

1285 Stern, S. A., et al. 2015. The Pluto system: Initial results from its exploration by New Horizons.  
1286 *Science* 350.6258, aad1815.

1287 Stevens, T.O., McKinley, J.P. 1995. Lithoautotrophic Microbia, Ecosystems in Deep Basalt  
1288 Aquifers. *Science* 270, 450-454.

1289 Stevenson, J. et al. 2015. Membrane alternatives in worlds without oxygen: Creation of an  
1290 azotosome. *Science advances* 1.1, e1400067.

1291 Stofan, E.R., and 37 colleagues 2007. The lakes of Titan. *Nature* 445, 61-64.

1292 Stofan, E., et al. 2013. TiME-the titan mare explorer. *IEEE aerospace conference* (pp. 1-10).

1293 Tajeddine, R. et al. 2017. True polar wander of Enceladus from topographic data. *Icarus*, 295, 46.

1294 Thomas, P.C., et al. 2016. Enceladus's measured physical libration requires a global subsurface  
1295 ocean. *Icarus* 264, 37-47.

1296 Thompson, W.R., Sagan, C. 1992. Organic chemistry on Titan: Surface interactions. Symposium  
1297 on Titan 338.

1298 Tobie, G., et al. 2005. Titan's internal structure inferred from a coupled thermal-orbital model.  
1299 *Icarus* 175, 496-502.

1300 Tobie, G., et al. 2006. Episodic outgassing as the origin of atmospheric methane on Titan. *Nature*  
1301 440, 61-64.

1302 Tobie, G., et al. 2012. Titan's Bulk Composition Constrained by Cassini-Huygens: Implication for  
1303 Internal Outgassing. *The Astrophysical Journal* 752, 125.

1304 Tomasko, M.G., and 39 colleagues 2005. Rain, winds and haze during the Huygens probe's descent  
1305 to Titan's surface. *Nature* 438, 765-778.

1306 Tomasko, M. G., and R. A. West. 2009. Aerosols in Titan's atmosphere. *Titan from Cassini-*  
1307 *Huygens*. Springer, Dordrecht, 297-321.

- 1308 Tortora, P. et al. 2017. Titan gravity investigation with the Oceanus mission. Geophysical  
1309 Research Abstracts, Vol. 19. EGU2017-17876.
- 1310 Tortora, P. et al. 2018. Titan gravity investigation from a SmallSat Satellite-to-Satellite Tracking  
1311 Mission. Geophysical Research Abstracts, Vol. 20, EGU2018-14126.
- 1312 Tortora, P. et al. 2018. Ocean Worlds Gravity Investigation using SmallSat Missions. In *42nd*  
1313 *COSPAR Scientific Assembly (Vol. 42)*.
- 1314 Turtle, E.P., and 13 colleagues 2011. Rapid and Extensive Surface Changes Near Titan's Equator:  
1315 Evidence of April Showers. *Science* 331, 1414.
- 1316 Vuitton, V., et al. 2007. Ion chemistry and N-containing molecules in Titan's upper atmosphere.  
1317 *Icarus* 191, 722-742.
- 1318 Yelle, R.V., et al. 2008. Methane escape from Titan's atmosphere. *Journal of Geophysical*  
1319 *Research (Planets)* 113, E10003.
- 1320 Yung, Y.L., et al. 1984. Photochemistry of the atmosphere of Titan - Comparison between model  
1321 and observations. *The Astrophysical Journal Supplement Series* 55, 465-506.
- 1322 Waite, J.H., and 13 colleagues 2006. Cassini Ion and Neutral Mass Spectrometer: Enceladus Plume  
1323 Composition and Structure. *Science* 311, 1419- 1422.
- 1324 Waite, J.H., et al. 2007. The Process of Tholin Formation in Titan's Upper Atmosphere. *Science*  
1325 316, 870.



1326 Waite, J.H., Jr., and 15 colleagues 2009. Liquid water on Enceladus from observations of ammonia  
1327 and 40Ar in the plume. *Nature* 460, 487- 490.

1328 Wilson, E.H., Atreya, S.K. 2009. Titan's Carbon Budget and the Case of the Missing Ethane.  
1329 *Journal of Physical Chemistry A* 113, 11221- 11226.

1330 Wood, C.A., et al. 2010, Impact craters on Titan. *Icarus* 206, 334–344.

1331 Zahnle, K., et al. 1992. Impact-generated atmospheres over Titan, Ganymede, and Callisto. *Icarus*  
1332 95, 1-23.

1333 Zahnle, K.J., et al. 2014. Transient climate effects of large impacts on Titan. *Icarus* 229, 378-391.

1334

1335

1336

1337

1338

1339

1340

1341

1342

1343 TABLES

1344 **Table 1.** Science goals of baseline mission

<b>Science summary</b>	
<b>Science goals</b>	<b>Science objectives</b>
Origin and evolution of volatile-rich ocean worlds, Enceladus and Titan	<ul style="list-style-type: none"><li>- Are Enceladus' volatile compounds primordial or have they been re-processed and if so, to what extent?</li><li>- What is the history and extent of volatile exchange on Titan?</li><li>- How has Titan's organic-rich surface evolved?</li></ul>
Habitability and potential for life of ocean worlds, Enceladus and Titan	<ul style="list-style-type: none"><li>- Is Enceladus' aqueous interior an environment favorable to the emergence of life?</li><li>- To what level of complexity has prebiotic chemistry evolved in the Titan system?</li></ul>

1345

1346

1347 **Table 2.** Science goals of optional sea probe (lander) element

<b>Science summary</b>	
<b>Science goals</b>	<b>Science objectives</b>
Origin and evolution of Titan's lakes and seas	<ul style="list-style-type: none"><li>- How does the hydrological cycle work, and what is the role of the lakes and seas? How have the seas and lakes evolved over time (e.g., shorelines)?</li><li>- Constrain the depth of a Titan sea</li><li>- What is the lower atmosphere over the sea?</li><li>- Constrain sea-atmosphere interactions</li></ul>
Habitability and potential for life of Titan's lakes and seas	<ul style="list-style-type: none"><li>- What is the composition of the seas and lakes?</li><li>- Are there any prebiotic or biotic signature compositions?</li><li>- What is the composition of evaporites and what is their relation to the lakes and seas?</li></ul>

1348

1349

1350

1351

1352 **Table 3.** Science goals of optional Ice Penetrating Radar (IPR) element

<b>Science summary</b>	
<b>Science goals</b>	<b>Science objectives</b>
Interior structure and processes of Enceladus and Titan	<ul style="list-style-type: none"><li>- What is the thickness of the surface organic material layer on Titan?</li><li>- How does ice thickness vary in Enceladus' south polar terrain?</li><li>- Constrain brittle-ductile transition within Titan's ice shell</li><li>- How do the surface and subsurface features correlate on Titan and Enceladus?</li><li>- Constrain the extent of Enceladus' ocean at SPT</li><li>- Constrain anomalous thermal emission beneath SPT</li><li>- What is the extent of surface and subsurface communication especially in the polar regions of both Titan and Enceladus?</li></ul>

1353

1354

1355

1356

1357

1358

1359

1360

1361

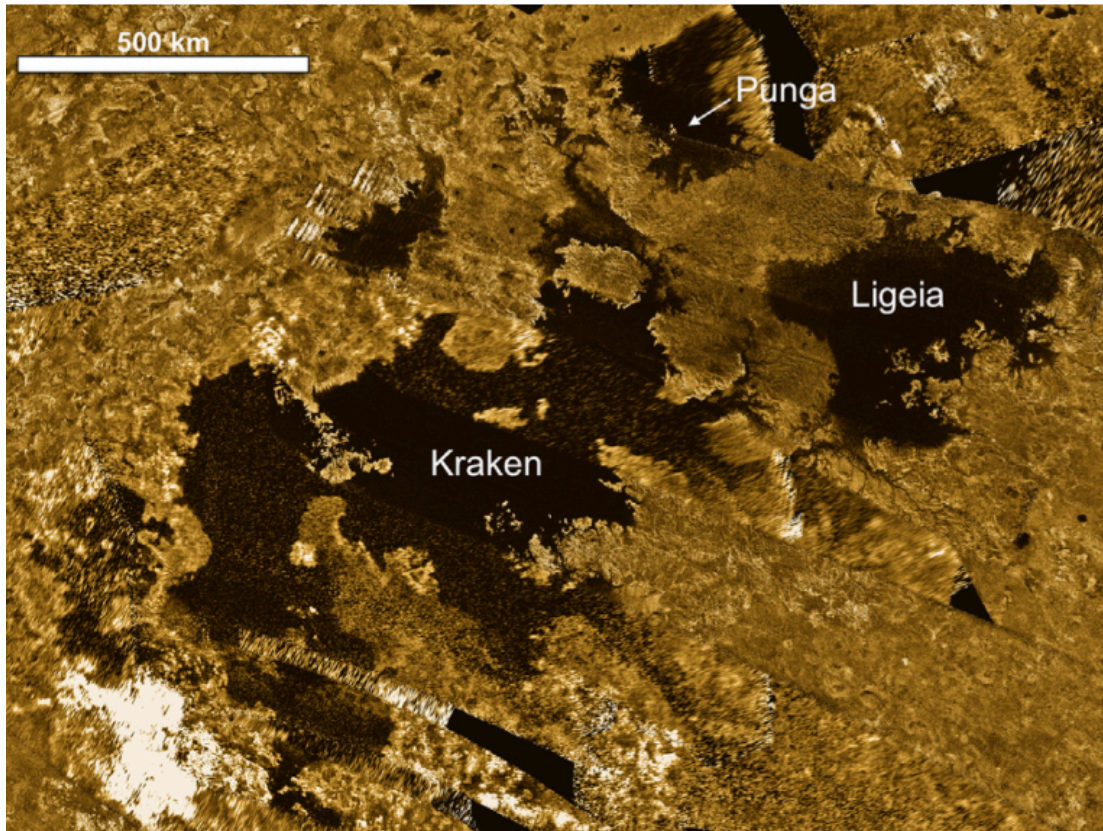
1362 **Table 4.** Science objectives, measurements and proposed techniques for option 1, the sea probe/lander  
 1363 (Mitri et al. 2014)

Science objectives		Measurements	Approaches and requirements
<b>Lakes/seas</b>	Characterize one of Titan's northern seas and its chemical composition (astrobiological potential)	Sea composition, including low and high mass hydrocarbons, noble gases, and carbon isotopes	Mass spectrometry Low atmosphere physical properties package (temperature sensor, barometer, anemometer)
		Exchange processes at the sea-air interface to help constrain the methane cycle	Low-atmosphere physical properties package (temperature sensor, barometer, anemometer)
		Presence and nature of waves and currents	Physical properties package
			Surface Imaging (~250 $\mu$ rad/pixel)
		Properties of sea liquids including turbidity and dielectric constant	Sea physical properties package (turbidity and dielectric constant measurements)
		Sea depths to constrain basin shape and sea volume	Sonar
		Shoreline characteristics, including evidence for past changes in sea level	Surface Imaging (~250 $\mu$ rad/pixel)
Surface Imaging (~250 $\mu$ rad/pixel)			
<b>Atmosphere</b>	Determine T, P, composition, evaporation rate and physical properties that characterize lake and atmosphere interactions	Determine T, P, composition, evaporation rate and physical properties that characterize lake and atmosphere interactions	Mass spectrometry Physical properties package
	Characterize the atmospheric composition during probe decent	Determine the composition	Mass spectrometry

1364

1365

1366

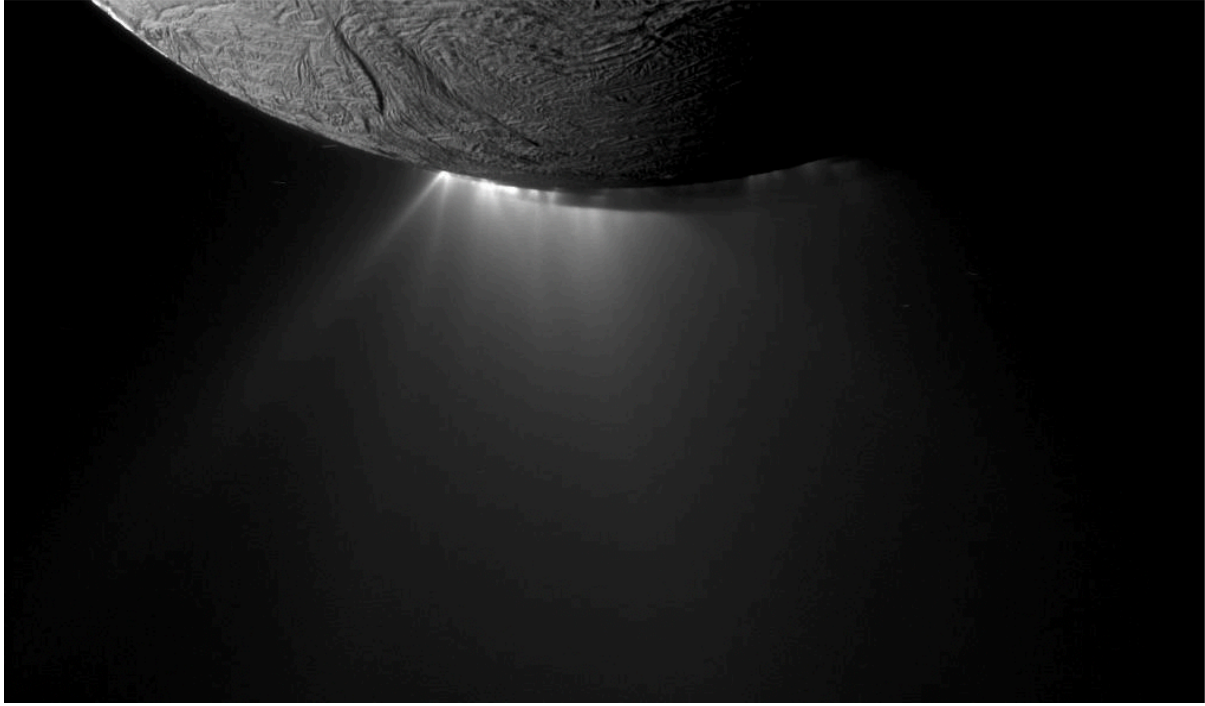


1368  
1369

1370 **Figure 1.** Cassini SAR mosaic images of the north polar region showing Kraken, Ligeia and Punga  
1371 Maria. Black–yellow color map was applied to the single band data (from Mitri et al. 2014a).

1372

1373



1374  
1375

1376 **Figure 2.** Plume emanating from multiple jets in Enceladus' south polar terrain.

1377

1378

1379

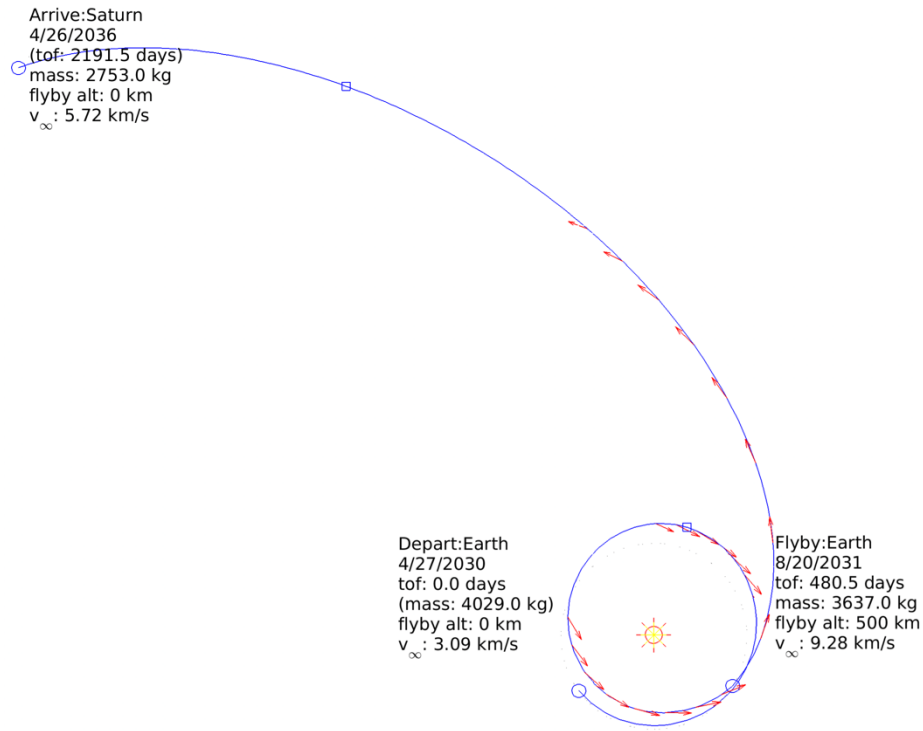
1380

1381

1382

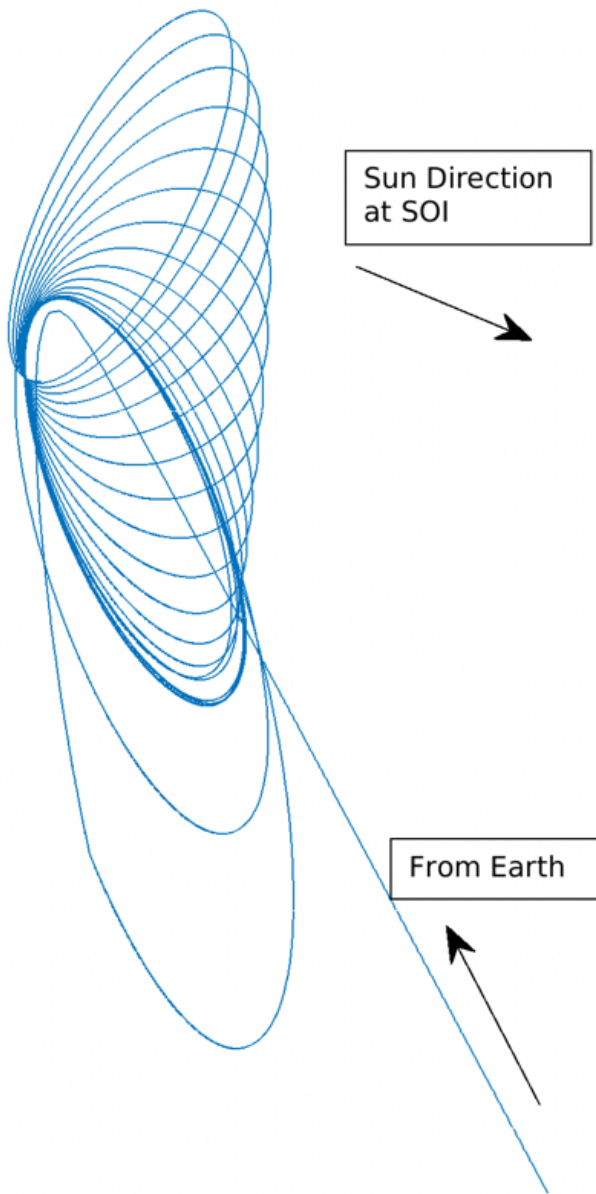
1383

1384



1385  
1386

1387 **Figure 3.** Example interplanetary transfer to Saturn studied for E<sup>2</sup>T proposal based on a proposed  
 1388 launch in 2029–2030 (Mitra et al. 2018). Red arrows indicate electric propulsion thrust. Such a  
 1389 scenario could be used to design a future transfer trajectory.



1390

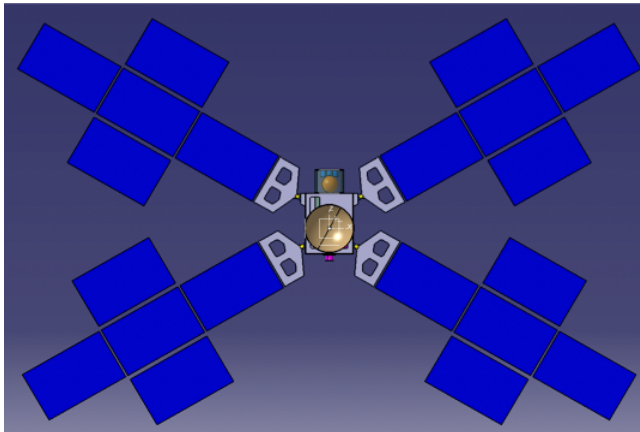
1391 **Figure 4.** Inertial representation of a sample tour based on a proposed 2029–2030 launch with two  
1392 period- and inclination-management Titan flybys followed by a science phase with 6 Enceladus  
1393 flybys and 17 Titan flybys (Mitri et al. 2018).

1394

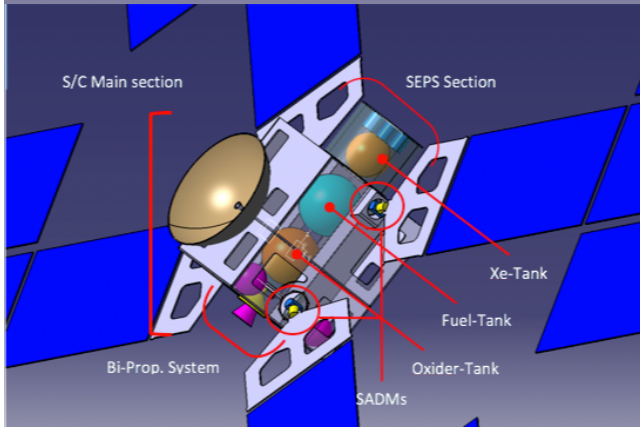
1395



1396



1397



1398

1399

1400 **Figure 5.** Proposed configuration of the S/C for the E<sup>2</sup>T project. Top panel shows an enlarged

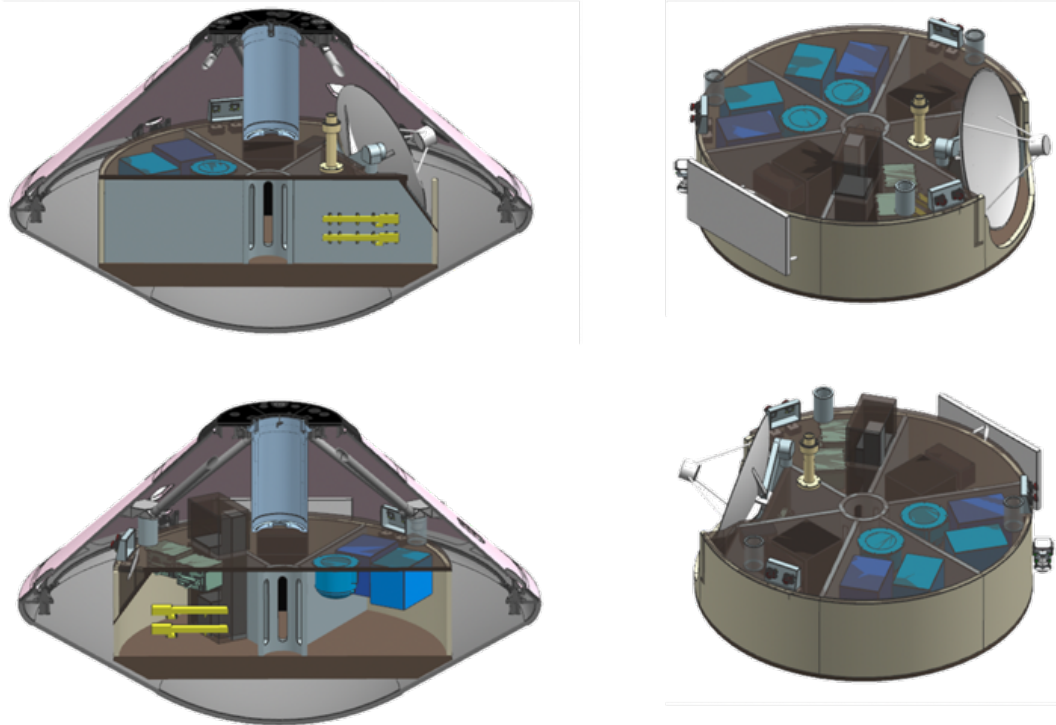
1401 view of the S/C and below panel shows a close-up view of the S/C (Mitri et al. 2018).

1402

1403

1404

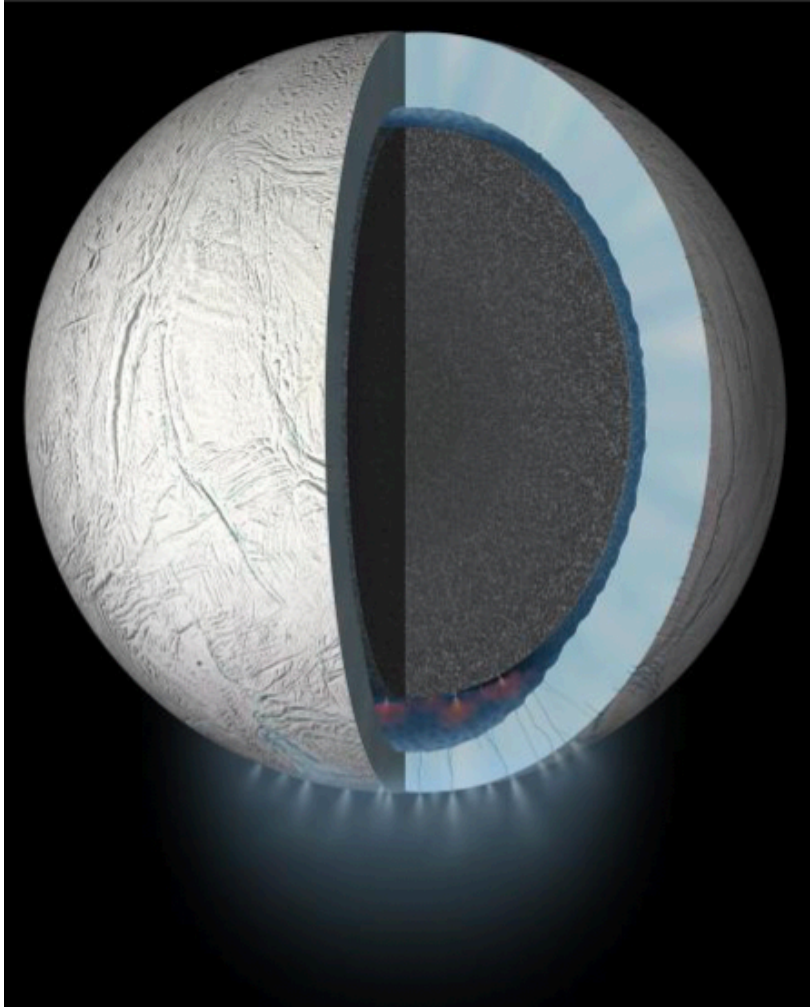
1405



1406

1407 **Figure 6.** Examples of a sea lander and entry vehicle. The right-hand panel shows front and back  
1408 views of the sea lander inside the entry vehicle while the left-hand panel shows the sea lander only.

1409 Credit: JPL.



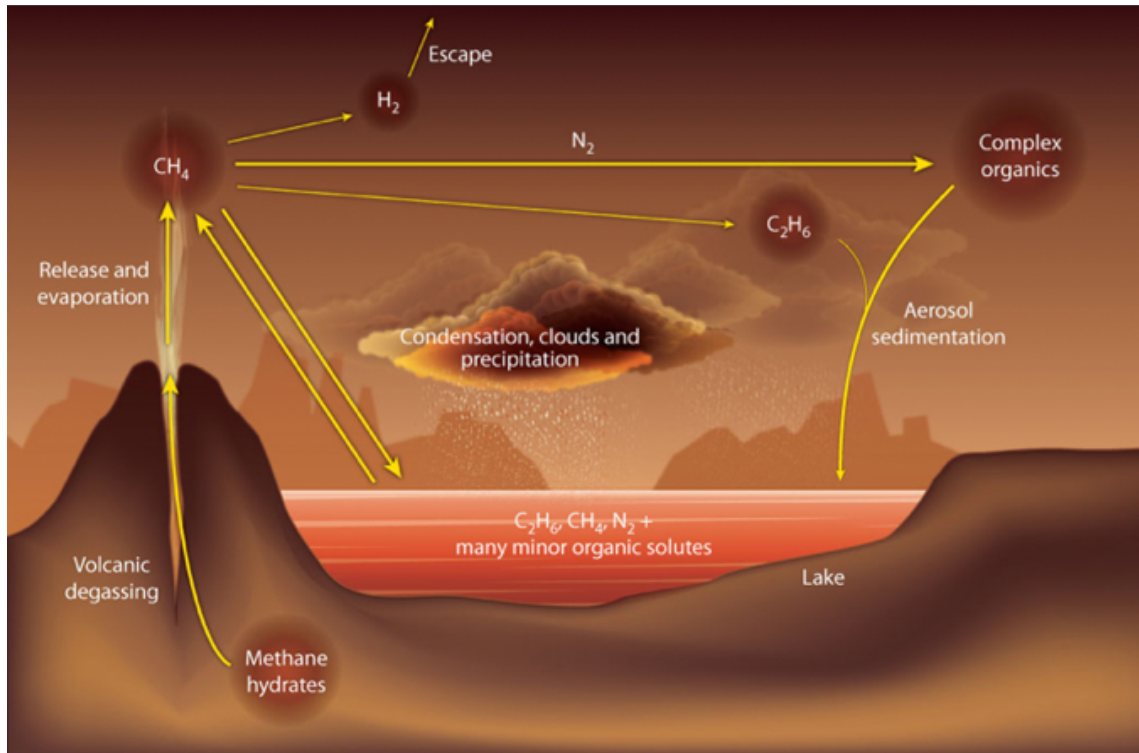
1410

1411 **Figure 7.** Enceladus' internal structure inferred from gravity, topography and libration  
1412 measurement provided by Cassini mission. A global subsurface ocean is present under the outer  
1413 ice shell. The ice shell is believed to be a few kilometers thin at the south polar region where the  
1414 center of the geological activity is with the formation of the plume formed by multi-jets.

1415

1416

1417



1418

1419 **Figure 8.** Titan's methanological cycle (Raulin, 2008).

1420

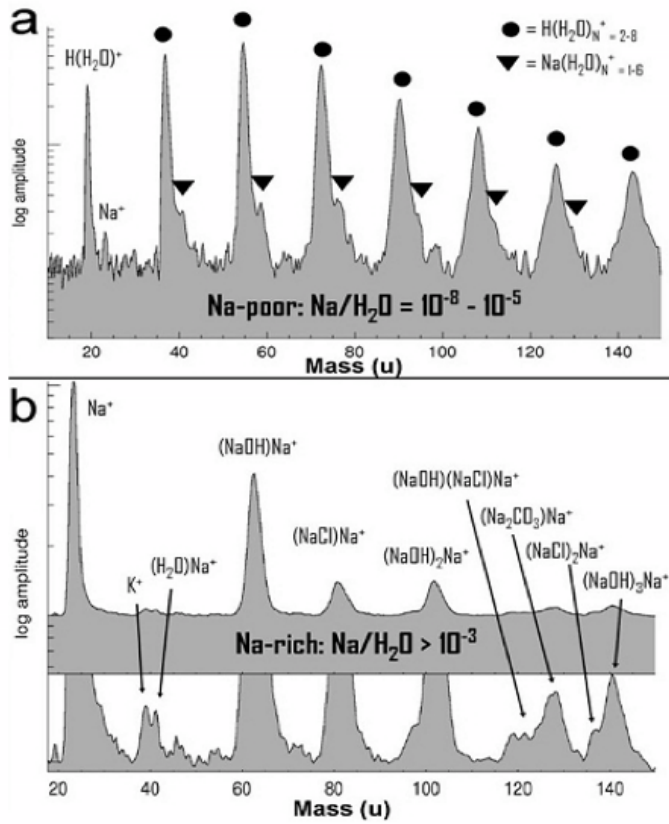
1421

1422

1423

1424

1425



1426

1427 **Figure 9.** Composition of salt-poor (Type I and II) and salt-rich (Type III) particles in Saturn's E-

1428 ring and Enceladus' plume (Postberg et al. 2011).